

# The thick-thin decomposition and the bilipschitz classification of normal surface singularities

by

LEV BIRBRAIR

*Universidade Federal do Ceará  
Fortaleza, Brasil*

WALTER D. NEUMANN

*Columbia University  
New York, U.S.A.*

ANNE PICHON

*Aix Marseille Université  
Marseille, France*

## Contents

1. Introduction . . . . .	200
2. Construction of the thick-thin decomposition . . . . .	206
3. Polar curves . . . . .	207
4. Milnor balls . . . . .	215
5. The thin pieces . . . . .	216
6. The thick pieces . . . . .	220
7. Fast loops . . . . .	221
8. Existence and uniqueness of the minimal thick-thin decomposition . . . . .	228
9. Metric tangent cone . . . . .	230
Part II: The bilipschitz classification . . . . .	231
10. The refined decomposition of $(X, 0)$ . . . . .	231
11. The bilipschitz model of $(X, 0)$ . . . . .	232
12. Carrousel decomposition and lifting . . . . .	235
13. Bilipschitz equivalence with the model . . . . .	238
14. Bilipschitz invariance of the data . . . . .	242
15. Examples . . . . .	245
References . . . . .	254

## 1. Introduction

Lipschitz geometry of complex singular spaces is an intensively developing subject. In [41], L. Siebenmann and D. Sullivan conjectured that the set of Lipschitz structures is tame, i.e., the set of equivalence classes of complex algebraic sets in  $\mathbb{C}^n$ , defined by polynomials of degree less than or equal to  $k$  is finite. One of the most important results on Lipschitz geometry of complex algebraic sets is the proof of this conjecture by T. Mostowski [30] (generalized to the real setting by Parusiński [35], [36]). But so far, there exists no explicit description of the equivalence classes, except in the case of complex plane curves which was studied by Pham–Teissier [38] and Fernandes [10]. They showed that the embedded Lipschitz geometry of plane curves is determined by the topology. The present paper is devoted to the case of complex algebraic surfaces, which is much richer.

Let  $(X, 0)$  be the germ of a normal complex surface singularity. Given an embedding  $(X, 0) \subset (\mathbb{C}^n, 0)$ , the standard hermitian metric on  $\mathbb{C}^n$  induces a metric on  $X$  given by arc-length of curves in  $X$  (the so-called “inner metric”). Up to bilipschitz equivalence, this metric is independent of the choice of embedding in affine space.

It is well known that for all sufficiently small  $\varepsilon > 0$  the intersection of  $X$  with the sphere  $S_\varepsilon \subset \mathbb{C}^n$  about 0 of radius  $\varepsilon$  is transverse, and the germ  $(X, 0)$  is therefore “topologically conical”, i.e., homeomorphic to the cone on its link  $X \cap S_\varepsilon$  (in fact, this is true for any semi-algebraic germ). However,  $(X, 0)$  need not be “metrically conical” (bilipschitz equivalent to a standard metric cone). The first example of a non-metrically-conical  $(X, 0)$  was given in [2], and the examples in [3]–[5] then suggested that failure of metric conicalness is common. In [5] it was also shown that bilipschitz geometry of a singularity may not be determined by its topology.

In those papers the failure of metric conicalness and differences in bilipschitz geometry were determined by local obstructions: existence of topologically non-trivial subsets of the link of the singularity (“fast loops” and “separating sets”) whose size shrinks faster than linearly as one approaches the origin.

In this paper we first describe a natural decomposition of the germ  $(X, 0)$  into two parts, the *thick* and the *thin* parts, such that the thin part carries all the “non-trivial” bilipschitz geometry, and we later refine this to give a classification of the bilipschitz structure. Our thick-thin decomposition is somewhat analogous to the Margulis thick-thin decomposition of a negatively curved manifold, where the thin part consists of points  $x$  which lie on a closed essential (i.e., non-null-homotopic) loop of length  $\leq 2\eta$  for some small  $\eta$ . A (rough) version of our thin part can be defined similarly using essential loops in  $X \setminus \{0\}$ , and with a length bound of the form  $\leq |x|^{1+c}$  for some small  $c$ . We return to this in §8.

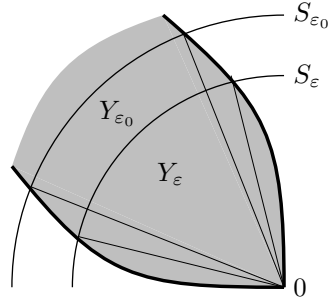


Figure 1. Thick germ.

*Definition 1.1.* (Thin) A semi-algebraic germ  $(Z, 0) \subset (\mathbb{R}^N, 0)$  of pure dimension  $k$  is *thin* if its tangent cone  $T_0Z$  has dimension strictly less than  $k$ .

This definition only depends on the inner metric of  $Z$  and not on the embedding in  $\mathbb{R}^N$ . Indeed, instead of  $T_0Z$  one can use the metric tangent cone  $\mathcal{T}_0Z$  of Bernig and Lytchak in the definition, since it is a bilipschitz invariant for the inner metric and maps finite-to-one to  $T_0Z$  (see [1]). The metric tangent cone is discussed further in §9, where we show that it can be recovered from the thick-thin decomposition.

“Thick” is a generalization of “metrically conical.” Roughly speaking, a thick algebraic set is obtained by slightly inflating a metrically conical set in order that it can interface along its boundary with thin parts. The precise definition is as follows.

*Definition 1.2.* (Thick) Let  $B_{\epsilon} \subset \mathbb{R}^N$  denote the ball of radius  $\epsilon$  centered at the origin, and  $S_{\epsilon}$  its boundary. A semi-algebraic germ  $(Y, 0) \subset (\mathbb{R}^N, 0)$  is *thick* if there exists  $\epsilon_0 > 0$  and  $K \geq 1$  such that  $Y \cap B_{\epsilon_0}$  is the union of subsets  $Y_{\epsilon}$ ,  $\epsilon \leq \epsilon_0$ , which are metrically conical with bilipschitz constant  $K$  and satisfy the following properties (see Figure 1):

- (1)  $Y_{\epsilon} \subset B_{\epsilon}$ ,  $Y_{\epsilon} \cap S_{\epsilon} = Y \cap S_{\epsilon}$  and  $Y_{\epsilon}$  is metrically conical as a cone on its link  $Y \cap S_{\epsilon}$ ;
- (2) for  $\epsilon_1 < \epsilon_2$  we have  $Y_{\epsilon_2} \cap B_{\epsilon_1} \subset Y_{\epsilon_1}$  and this embedding respects the conical structures; moreover, the difference  $(Y_{\epsilon_1} \cap S_{\epsilon_1}) \setminus (Y_{\epsilon_2} \cap S_{\epsilon_1})$  of the links of these cones is homeomorphic to  $\partial(Y_{\epsilon_1} \cap S_{\epsilon_1}) \times [0, 1)$ .

Clearly, a semi-algebraic germ cannot be both thick and thin. The following proposition helps picture “thinness”. Although it is well known, we give a quick proof in §5 for convenience.

Let  $1 < q \in \mathbb{Q}$ . A *q-horn neighborhood* of a semi-algebraic germ  $(A, 0) \subset (\mathbb{R}^N, 0)$  is a set of the form  $\{x \in \mathbb{R}^n \cap B_{\epsilon} : d(x, A) \leq c|x|^q\}$  for some  $c > 0$ .

**PROPOSITION 1.3.** *Any semi-algebraic germ  $(Z, 0) \subset (\mathbb{R}^N, 0)$  is contained in some q-horn neighborhood of its tangent cone  $T_0Z$ .*

For example, the set  $Z = \{(x, y, z) \in \mathbb{R}^3 : x^2 + y^2 \leq z^3\}$  gives a thin germ at 0 since it is a 3-dimensional germ whose tangent cone is the  $z$ -axis. The intersection  $Z \cap B_\varepsilon$  is contained in a closed  $\frac{3}{2}$ -horn neighborhood of the  $z$ -axis. The complement in  $\mathbb{R}^3$  of this thin set is thick.

For any subgerm  $(A, 0)$  of  $(\mathbb{C}^n, 0)$  or  $(\mathbb{R}^N, 0)$  we write

$$A^{(\varepsilon)} := A \cap S_\varepsilon \subset S_\varepsilon.$$

In particular, when  $A$  is semi-algebraic and  $\varepsilon$  is sufficiently small,  $A^{(\varepsilon)}$  is the  $\varepsilon$ -link of  $(A, 0)$ .

*Definition 1.4.* (Thick-thin decomposition) A *thick-thin decomposition* of the normal complex surface germ  $(X, 0)$  is a decomposition of it as a union of germs of pure dimension 4:

$$(X, 0) = \bigcup_{i=1}^r (Y_i, 0) \cup \bigcup_{j=1}^s (Z_j, 0), \quad (1.1)$$

such that the  $Y_i \setminus \{0\}$  and  $Z_j \setminus \{0\}$  are connected and

- (1) each  $Y_i$  is thick and each  $Z_j$  is thin;
- (2) the  $Y_i \setminus \{0\}$  are pairwise disjoint and the  $Z_j \setminus \{0\}$  are pairwise disjoint;
- (3) if  $\varepsilon_0$  is chosen so small that  $S_\varepsilon$  is transverse to each of the germs  $(Y_i, 0)$  and  $(Z_j, 0)$  for  $\varepsilon \leq \varepsilon_0$ , then  $X^{(\varepsilon)} = \bigcup_{i=1}^r Y_i^{(\varepsilon)} \cup \bigcup_{j=1}^s Z_j^{(\varepsilon)}$  decomposes the 3-manifold  $X^{(\varepsilon)} \subset S_\varepsilon$  into connected submanifolds with boundary, glued along their boundary components.

We call the links  $Y_i^{(\varepsilon)}$  and  $Z_j^{(\varepsilon)}$  of the thick and thin pieces *thick* and *thin zones* of the link  $X^{(\varepsilon)}$ .

*Definition 1.5.* A thick-thin decomposition is *minimal* if

- (1) the tangent cone of its thin part  $\bigcup_{j=1}^s Z_j$  is contained in the tangent cone of the thin part of any other thick-thin decomposition;
- (2) the number  $s$  of its thin pieces is minimal among thick-thin decompositions satisfying (1).

The following theorem expresses the existence and uniqueness of a minimal thick-thin decomposition for a normal complex surface germ  $(X, 0)$ .

**THEOREM 1.6.** *A minimal thick-thin decomposition of  $(X, 0)$  exists. For any two minimal thick-thin decompositions of  $(X, 0)$  there exists  $q > 1$  and a homeomorphism of the germ  $(X, 0)$  to itself which takes one decomposition to the other and moves each  $x \in X$  a distance at most  $|x|^q$ .*

The homeomorphism in the above theorem is not necessarily bilipschitz, but the bilipschitz classification which we describe later leads to a “best” minimal thick-thin decomposition, which is unique up to bilipschitz homeomorphism.

THEOREM 1.7. (Properties) *A minimal thick-thin decomposition of  $(X, 0)$  as in equation (1.1) satisfies  $r \geq 1$ ,  $s \geq 0$  and has the following properties for  $0 < \varepsilon \leq \varepsilon_0$ :*

- (1) *each thick zone  $Y_i^{(\varepsilon)}$  is a Seifert fibered manifold;*
- (2) *each thin zone  $Z_j^{(\varepsilon)}$  is a graph manifold (a union of Seifert manifolds glued along boundary components) but not a solid torus;*
- (3) *there exist constants  $c_j > 0$  and  $q_j > 1$  and fibrations  $\zeta_j^{(\varepsilon)}: Z_j^{(\varepsilon)} \rightarrow S^1$  depending smoothly on  $\varepsilon \leq \varepsilon_0$  such that the fibers  $\zeta_j^{-1}(t)$  have diameter at most  $c_j \varepsilon^{q_j}$  (we call these fibers the Milnor fibers of  $Z_j^{(\varepsilon)}$ ).*

The minimal thick-thin decomposition is constructed in §2. Its minimality and uniqueness are proved in §8.

We will take a resolution approach to construct the thick-thin decomposition, but another way of constructing it is as follows. Recall (see [42] and [23]) that a line  $L$  tangent to  $X$  at 0 is *exceptional* if the limit at 0 of tangent planes to  $X$  along a curve in  $X$  tangent to  $L$  at 0 depends on the choice of this curve. Only finitely many tangent lines to  $X$  at 0 are exceptional. To obtain the thin part one intersects  $X \setminus \{0\}$  with a  $q$ -horn disk-bundle neighborhood of each exceptional tangent line  $L$  for  $q > 1$  sufficiently small and then discards any “trivial” components of these intersections (those whose closures are locally just cones on solid tori; such trivial components arise also in our resolution approach, and showing that they can be absorbed into the thick part takes some effort, see §6).

In [3] a *fast loop* is defined as a family of closed curves in the links  $X^{(\varepsilon)} := X \cap S_\varepsilon$ ,  $0 < \varepsilon \leq \varepsilon_0$ , depending continuously on  $\varepsilon$ , which are not homotopically trivial in  $X^{(\varepsilon)}$  but whose lengths are proportional to  $\varepsilon^k$  for some  $k > 1$ , and it is shown that fast loops are obstructions to metric conicalness.<sup>(1)</sup>

In Theorem 7.5 we show the following result.

THEOREM. (Theorem 7.5) *Each thin piece  $Z_j$  contains fast loops. In fact, each boundary component of its Milnor fiber gives a fast loop.*

COROLLARY 1.8. *The following are equivalent, and each implies that the link of  $(X, 0)$  is Seifert fibered:*

- (1)  *$(X, 0)$  is metrically conical;*
- (2)  *$(X, 0)$  has no fast loops;*
- (3)  *$(X, 0)$  has no thin piece (so it consists of a single thick piece).*

---

<sup>(1)</sup> We later call these *fast loops of the first kind*, since in §7 we define a related concept of *fast loop of the second kind* and show that these also obstruct metric conicalness.

**Bilipschitz classification.** We will give a complete classification of the geometry of  $(X, 0)$  up to bilipschitz equivalence, based on a refinement of the thick-thin decomposition. We will describe this refinement in terms of the decomposition of the link  $X^{(\varepsilon)}$ .

We first refine the decomposition

$$X^{(\varepsilon)} = \bigcup_{i=1}^r Y_i^{(\varepsilon)} \cup \bigcup_{j=1}^s Z_j^{(\varepsilon)}$$

by decomposing each thin zone  $Z_j^{(\varepsilon)}$  into its JSJ decomposition (minimal decomposition into Seifert fibered manifolds glued along their boundaries [17], [34]), while leaving the thick zones  $Y_i^{(\varepsilon)}$  as they are. We then thicken some of the gluing tori of this refined decomposition to collars  $T^2 \times I$ , to add some extra “annular” pieces (the choice where to do this is described in §10). At this point we have  $X^{(\varepsilon)}$  glued together from various Seifert fibered manifolds (in general not the minimal such decomposition).

Let  $\Gamma_0$  be the decomposition graph for this, with a vertex for each piece and edge for each gluing torus, so we can write this decomposition as

$$X^{(\varepsilon)} = \bigcup_{\nu \in V(\Gamma_0)} M_\nu^{(\varepsilon)}, \quad (1.2)$$

where  $V(\Gamma_0)$  is the vertex set of  $\Gamma_0$ .

**THEOREM 1.9.** (Classification theorem) *The bilipschitz geometry of  $(X, 0)$  determines and is uniquely determined by the following data:*

- (1) *the decomposition of  $X^{(\varepsilon)}$  into Seifert fibered manifolds as described above, refining the thick-thin decomposition;*
- (2) *for each thin zone  $Z_j^{(\varepsilon)}$ , the homotopy class of the foliation by fibers of the fibration  $\zeta_j^{(\varepsilon)}: Z_j^{(\varepsilon)} \rightarrow S^1$  (see Theorem 1.7 (3));*
- (3) *for each vertex  $\nu \in V(\Gamma_0)$ , a rational weight  $q_\nu \geq 1$  with  $q_\nu = 1$  if and only if  $M_\nu^{(\varepsilon)}$  is a  $Y_i^{(\varepsilon)}$  (i.e., a thick zone), and with  $q_\nu \neq q_{\nu'}$  if  $\nu$  and  $\nu'$  are adjacent vertices.*

In item (2) we ask for the foliation by fibers rather than the fibration itself since we do not want to distinguish fibrations  $\zeta: Z \rightarrow S^1$  which become equivalent after composing each with a covering map  $S^1 \rightarrow S^1$ . Note that item (2) describes discrete data, since the foliation is determined up to homotopy by a primitive element of  $H^1(Z_j^{(\varepsilon)}; \mathbb{Z})$  up to sign.

The data of the above theorem can also be conveniently encoded by adding the  $q_\nu$ 's as weights on a suitable decorated resolution graph. We do this in §15, where we compute various examples.

The proof of Theorem 1.9 is in terms of a canonical “bilipschitz model”

$$\widehat{X} = \bigcup_{\nu \in V(\Gamma_0)} \widehat{M}_\nu \cup \bigcup_{\sigma \in E(\Gamma_0)} \widehat{A}_\sigma, \quad (1.3)$$

with  $\widehat{X} \cong X \cap B_\varepsilon$  (bilipschitz) and where each  $\widehat{A}_\sigma$  is a *collar* (a cone on a toral annulus  $T^2 \times I$ ), while each  $\widehat{M}_\nu$  is homeomorphic to the cone on  $M_\nu^{(\varepsilon)}$ . The pieces carry Riemannian metrics determined by the  $q_\nu$ 's and the foliation data of the theorem; these metrics are global versions of the local metrics used by Hsiang–Pati [16] and Nagase [32]. On a piece  $\widehat{M}_\nu$  the metric is what Hsiang and Pati call a “Cheeger-type metric” (locally of the form  $dr^2 + r^2 d\theta^2 + r^{2q_\nu} (dx^2 + dy^2)$ ; see Definitions 11.2 and 11.3). On a piece  $\widehat{A}_\sigma$  it has a Nagase-type metric as described in Nagase’s correction to [16] (see Definition 11.1).

Mostowski’s work [30] mentioned above is based on a construction of Lipschitz trivial stratifications. Our approach is different in that we decompose the germ  $(X, 0)$  using the carousel theory of D. T. Lê [19] (see also [21]) applied to the discriminant curve of a generic plane projection of the surface. However, our work has some similarities with Mostowski’s (loc. cit., see also [31]) in the sense that the geometry near the polar curves also plays an important role, in particular the subgerms where the family of polar curves accumulates while one varies the direction of projections (Propositions 3.3 and 3.4).

A thick-thin decomposition exists also for higher-dimensional germs, and we conjecture with Alberto Verjovsky that it can be made canonical. It is the rigidity of topology in dimension 3, linked to the non-triviality of fundamental groups in this dimension, which enables us to get strong results for surfaces. The less rigid topology in higher dimensions makes it harder to pin down the “trivial” parts mentioned earlier which can be absorbed into the thick zones, and there are similar issues in determining boundaries between the pieces in a full bilipschitz classification.

**Acknowledgments.** We are very grateful to the referee for insightful comments which corrected an error in the paper and improved it in other ways, and to A. Parusiński, J. Snoussi, D. O’Shea, B. Teissier, G. Valette, and A. Verjovsky for useful conversations. Neumann was supported by NSF grants DMS-0905770 and DMS-1206760. Birbrair was supported by CNPq grants 201056/2010-0 and 300575/2010-6. Pichon was supported by the ANR project SUSI 12-JS01-0002-01. We are also grateful for the hospitality/support of the following institutions: Jagiellonian University (B), Columbia University (B, P), Institut de Mathématiques de Luminy, Université d’Aix-Marseille, Instituto do Milénio (N), IAS Princeton, CIRM petit groupe de travail (B, N, P), Universidade Federal do Ceará, CRM Montréal (N, P).

## 2. Construction of the thick-thin decomposition

Let  $(X, 0) \subset (\mathbb{C}^n, 0)$  be a normal surface germ. In this section, we explicitly describe the thick-thin decomposition for a normal complex surface germ  $(X, 0)$  in terms of a suitably adapted resolution of  $(X, 0)$ .

Let  $\pi: (\tilde{X}, E) \rightarrow (X, 0)$  be the minimal resolution with the following properties:

(1) It is a good resolution, i.e., the exceptional divisors are smooth and meet transversely, at most two at a time.

(2) It has no basepoints for a general linear system of hyperplane sections, i.e.,  $\pi$  factors through the normalized blow-up of the origin. An exceptional curve intersecting the strict transforms of the generic members of a general linear system will be called an  $\mathcal{L}$ -curve.

(3) No two  $\mathcal{L}$ -curves intersect.

This is achieved by starting with a minimal good resolution, then blowing up to resolve any basepoints of a general system of hyperplane sections, and finally blowing up any intersection point between  $\mathcal{L}$ -curves.

Let  $\Gamma$  be the resolution graph of the above resolution. A vertex of  $\Gamma$  is called a *node* if it has valency  $\geq 3$  or represents a curve of genus  $> 0$  or represents an  $\mathcal{L}$ -curve. If a node represents an  $\mathcal{L}$ -curve it is called an  $\mathcal{L}$ -node, otherwise a  $\mathcal{T}$ -node. By the previous paragraph,  $\mathcal{L}$ -nodes cannot be adjacent to each other.

The subgraphs of  $\Gamma$  resulting after removing the  $\mathcal{L}$ -nodes and adjacent edges from  $\Gamma$  are called the *Tjurina components* of  $\Gamma$  (following [43, Definition III.3.1]), so  $\mathcal{T}$ -nodes are precisely the nodes of  $\Gamma$  that are in Tjurina components.

A *string* is a connected subgraph of  $\Gamma$  containing no nodes. A *bamboo* is a string ending in a vertex of valence 1.

For each exceptional curve  $E_\nu$  in  $E$  let  $N(E_\nu)$  be a small closed tubular neighborhood. For any subgraph  $\Gamma'$  of  $\Gamma$  define (see Figure 2)

$$N(\Gamma') := \bigcup_{\nu \in \Gamma'} N(E_\nu) \quad \text{and} \quad \mathcal{N}(\Gamma') := \overline{N(\Gamma) \setminus \bigcup_{\nu \notin \Gamma'} N(E_\nu)}.$$

In the introduction we used standard  $\varepsilon$ -balls to state our results, but in practice it is often more convenient to work with a different family of Milnor balls. For example, one can use, as in Milnor [29], the ball of radius  $\varepsilon$  at the origin, or the balls with corners introduced by Kähler [18], Durfee [8] and others. In our proofs it will be convenient to use balls with corners, but it is a technicality to deduce the results for round Milnor balls. We will define the specific family of balls we use in §4. We denote it again by  $B_\varepsilon$ ,  $0 < \varepsilon \leq \varepsilon_0$ , and put  $S_\varepsilon := \partial B_\varepsilon$ .



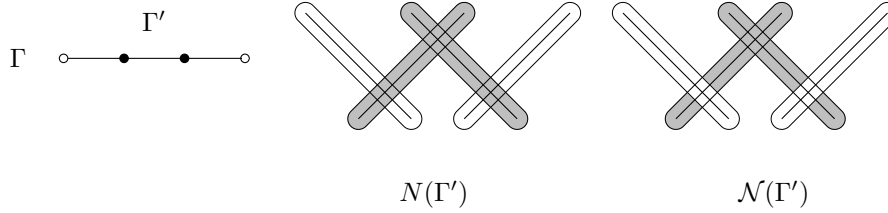


Figure 2.  $N(\Gamma')$  and  $\mathcal{N}(\Gamma')$  for the  $A_4$  singularity.

*Definition 2.1.* (Thick-thin decomposition) Let  $\varepsilon_0$  be so small that  $\pi^{-1}(X \cap B_{\varepsilon_0})$  is included in  $N(\Gamma)$ . Let  $\Gamma_1, \dots, \Gamma_s$  denote the Tjurina components of  $\Gamma$  which are not bamboos, and  $\Gamma'_1, \dots, \Gamma'_r$  be the maximal connected subgraphs in  $\Gamma \setminus \bigcup_{j=1}^s \Gamma_j$ .

For each  $i=1, \dots, r$ , define

$$Y_i := \pi(N(\Gamma'_i)) \cap B_{\varepsilon_0},$$

and for each  $j=1, \dots, s$ , define

$$Z_j := \pi(\mathcal{N}(\Gamma_j)) \cap B_{\varepsilon_0}.$$

Notice that each  $\Gamma'_i$  consists of an  $\mathcal{L}$ -node and any attached bamboos. So the  $Y_i$  are in one-to-one correspondence with the  $\mathcal{L}$ -nodes.

The  $Y_i$  are the *thick pieces* and the  $Z_j$  are the *thin pieces*.

By construction, the decomposition

$$(X, 0) = \bigcup_{j=1}^s (Z_j, 0) \cup \bigcup_{i=1}^r (Y_i, 0)$$

satisfies items (2) and (3) of Definition 1.4 and items (1) and (2) of Theorem 1.7. Item (3) of Theorem 1.7 and the thinness of the  $Z_j$  are proved in §5. The thickness of  $Y_i$  is proved in §6.

### 3. Polar curves

Let  $(X, 0) \subset (\mathbb{C}^n, 0)$  be a normal surface germ. In this section, we prove two independent results on polar curves of linear projections  $X \rightarrow \mathbb{C}^2$  which will be used in the sequel. We first need to introduce some classical material.

Let  $\mathcal{D}$  be an  $(n-2)$ -plane in  $\mathbb{C}^n$  and let  $\ell_{\mathcal{D}}: \mathbb{C}^n \rightarrow \mathbb{C}^2$  be the linear projection  $\mathbb{C}^n \rightarrow \mathbb{C}^2$  with kernel  $\mathcal{D}$ . We restrict ourselves to those  $\mathcal{D}$  in the Grassmanian  $\mathbf{G}(n-2, \mathbb{C}^n)$  such

that the restriction  $\ell_{\mathcal{D}}|_{(X,0)}: (X,0) \rightarrow (\mathbb{C}^2,0)$  is finite. The *polar curve*  $\Pi_{\mathcal{D}}$  of  $(X,0)$  for the direction  $\mathcal{D}$  is the closure in  $(X,0)$  of the singular locus of the restriction of  $\ell_{\mathcal{D}}$  to  $X \setminus \{0\}$ . The *discriminant curve*  $\Delta_{\mathcal{D}} \subset (\mathbb{C}^2,0)$  is the image  $\ell_{\mathcal{D}}(\Pi_{\mathcal{D}})$  of the polar curve  $\Pi_{\mathcal{D}}$ .

There exists an open dense subset  $\Omega \subset \mathbf{G}(n-2, \mathbb{C}^n)$  such that the germs of curves  $(\Pi_{\mathcal{D}}, 0)$ ,  $\mathcal{D} \in \Omega$ , are equisingular in terms of strong simultaneous resolution and such that the discriminant curves  $\Delta_{\mathcal{D}} = \ell_{\mathcal{D}}(\Pi_{\mathcal{D}})$  are reduced and no tangent line to  $\Pi_{\mathcal{D}}$  at 0 is contained in  $\mathcal{D}$  ([22, paragraph (2.2.2)] and [45, Chapter V, 1.2.2 Lemme-clé]).

The condition  $\Delta_{\mathcal{D}}$  reduced means that any  $p \in \Delta_{\mathcal{D}} \setminus \{0\}$  has a neighborhood  $U$  in  $\mathbb{C}^2$  such that one component of  $(\ell_{\mathcal{D}}|_X)^{-1}(U)$  maps by a two-fold branched cover to  $U$  and the other components map bijectively.

*Definition 3.1.* The projection  $\ell_{\mathcal{D}}: \mathbb{C}^n \rightarrow \mathbb{C}^2$  is *generic* for  $(X,0)$  if  $\mathcal{D} \in \Omega$ .

Let  $\lambda: X \setminus \{0\} \rightarrow \mathbf{G}(2, \mathbb{C}^n)$  be the map which maps  $x \in X \setminus \{0\}$  to the tangent plane  $T_x X$ . The closure  $\tilde{X}$  of the graph of  $\lambda$  in  $X \times \mathbf{G}(2, \mathbb{C}^n)$  is a reduced analytic surface. By definition, the *Nash modification* of  $(X,0)$  is the induced morphism  $\nu: \tilde{X} \rightarrow X$ .

LEMMA 3.2. ([43, Part III, Theorem 1.2], [11, §2]) *A resolution of  $(X,0)$  factors through Nash modification if and only if it has no base points for the family of polar curves.*

Let us fix  $\mathcal{D} \in \Omega$ . We suppress the subscript  $\mathcal{D}$  and denote simply  $\ell$  for  $\ell_{\mathcal{D}}$  and  $\Pi$  and  $\Delta$  for the polar and discriminant curves of  $\ell|_X$ . The *local bilipschitz constant* of  $\ell|_X$  is the map  $K: X \setminus \{0\} \rightarrow \mathbb{R} \cup \{\infty\}$  defined as follows. It is infinite on the polar curve and at a point  $p \in X \setminus \Pi$  it is the reciprocal of the shortest length among images of unit vectors in  $T_p X$  under the projection  $d\ell: T_p X \rightarrow \mathbb{C}^2$ .

PROPOSITION 3.3. *Let  $\pi': \tilde{X}' \rightarrow X$  be a resolution of  $X$  which factors through Nash modification. Let  $\Pi^*$  denote the strict transform of the polar curve  $\Pi$  by  $\pi'$ . Given any neighborhood  $U$  of  $\Pi^* \cap (\pi')^{-1}(B_\varepsilon \cap X)$  in  $\tilde{X}' \cap (\pi')^{-1}(B_\varepsilon \cap X) \setminus C$ , the local bilipschitz constant  $K$  is bounded on  $(B_\varepsilon \cap X) \setminus \pi'(U)$ .*

*Proof.* Let  $\sigma: \tilde{X}' \rightarrow \mathbf{G}(2, \mathbb{C}^n)$  be the map induced by the projection

$$p_2: \tilde{X}' \subset X \times \mathbf{G}(2, \mathbb{C}^n) \longrightarrow \mathbf{G}(2, \mathbb{C}^n),$$

and let  $\alpha: \mathbf{G}(2, \mathbb{C}^n) \rightarrow \mathbb{R} \cup \{\infty\}$  be the map sending  $H \in \mathbf{G}(2, \mathbb{C}^n)$  to the bilipschitz constant of the restriction  $\ell|_H: H \rightarrow \mathbb{C}^2$ . The map  $\alpha \circ \sigma$  coincides with  $K \circ \pi'$  on  $\tilde{X}' \setminus (\pi')^{-1}(0)$  and takes finite values outside  $\Pi^*$ . The map  $\alpha \circ \sigma$  is continuous and therefore bounded on the compact set  $(\pi')^{-1}(B_\varepsilon) \setminus U$ .  $\square$

In the rest of the section, we consider a branch  $\Delta_0$  of the discriminant curve  $\Delta$  and the component  $\Pi_0$  of the polar of  $\ell$  such that  $\ell(\Pi_0)=\Delta_0$ . We will study the behavior of  $\ell$  on a suitable zone  $A$  in  $X$  containing  $\Pi_0$ , outside of which  $\ell$  is a local bilipschitz homeomorphism.

We choose coordinates in  $\mathbb{C}^2$  so that  $\Delta_0$  is not tangent to the  $y$ -axis. Then  $\Delta_0$  admits a Puiseux series expansion

$$y = \sum_{j \geq 1} a_j x^{p_j} \in \mathbb{C}\{x^{1/N}\}, \quad \text{with } p_j \in \mathbb{Q} \text{ and } 1 \leq p_1 < p_2 < \dots$$

Here  $N = \text{lcm}_{j \geq 1} \text{denom}(p_j)$ , where “denom” means denominator.

For  $K_0 \geq 1$ , set  $B_{K_0} := \{p \in X \cap (B_\varepsilon \setminus \{0\}) : K(p) \geq K_0\}$ , and let  $B_{K_0}(\Pi_0)$  denote the closure of the connected component of  $B_{K_0} \setminus \{0\}$  which contains  $\Pi_0 \setminus \{0\}$ . We set

$$N_{K_0}(\Delta_0) = \ell(B_{K_0}(\Pi_0)).$$

PROPOSITION 3.4. (Polar wedge lemma)

(1) *There exists  $k \geq 1$  such that if  $s = p_k$  then for any  $\alpha > 0$  there is  $K_0 \geq 1$  such that  $N_{K_0}(\Delta_0)$  is contained in the set*

$$B = \left\{ (x, y) : \left| y - \sum_{j \geq 1} a_j x^{p_j} \right| \leq \alpha |x|^s \right\}.$$

We call the largest such  $s$  the contact exponent of  $\Delta_0$ .

(2) *Let  $A_0$  be the closure of the component of  $\ell^{-1}(B) \setminus \{0\}$  which contains  $\Pi_0$ . Then, up to bilipschitz equivalence,  $A_0$  is a topological cone on a solid torus,*

$$([0, \varepsilon] \times S^1 \times D^2) / (\{0\} \times S^1 \times D^2),$$

equipped with the metric  $dr^2 + r^2 d\theta^2 + r^{2s} g$ , where  $g$  is the standard metric on the unit disk. We call such an  $A_0$  a polar wedge.

*Remark.* Note that, in part (1),  $B$  could be replaced by the set

$$B' = \left\{ (x, y) : \left| y - \sum_{\substack{j \geq 1 \\ p_j \leq s}} a_j x^{p_j} \right| \leq \alpha |x|^s \right\},$$

since truncating higher-order terms does not change the bilipschitz geometry. Up to bilipschitz equivalence, this does not change  $A_0$  in part (2) either.

*Proof.* We are considering the germ  $(X, 0)$ , so in this proof all subsets of  $X$  or  $\tilde{X}'$  are implicitly intersected with  $B_\varepsilon$  or  $(\pi')^{-1}(B_\varepsilon)$  for some sufficiently small  $\varepsilon$ .

According to Proposition 3.3, for each neighborhood  $A^*$  of  $\Pi_0^*$  in  $\tilde{X}'$  there exists  $K_0$  such that  $B_{K_0}(\Pi_0) \subset \pi'(A^*)$ . We first construct such an  $A^*$  as the union of a family of disjoint strict transforms of components  $\Pi_{0, \mathcal{D}_t}^*$  of polars  $\Pi_{\mathcal{D}_t}^*$  parameterized by  $t$  in a neighborhood of 0 in  $\mathbb{C}$ , and with  $\mathcal{D}_0 = \mathcal{D}$ . So  $\Pi_0 = \Pi_{0, \mathcal{D}_0}$ . Let  $E \subset (\pi')^{-1}(0)$  be the exceptional curve with  $E \cap \Pi_0^* \neq \emptyset$ .

Let  $\sigma: \tilde{X}' \rightarrow \mathbf{G}(2, \mathbb{C}^n)$  be as in the proof of Proposition 3.3 and let  $U$  denote a small neighborhood of  $T := \sigma(E \cap \Pi_0^*)$  in  $\mathbf{G}(2, \mathbb{C}^n)$ . We first assume that  $n=3$ , so

$$\mathbf{G}(2, \mathbb{C}^n) = \mathbf{G}(2, \mathbb{C}^3) \cong P^2\mathbb{C}.$$

Choose any  $T' \in \mathbf{G}(2, \mathbb{C}^3) \setminus U$  so that  $T' \subset \mathbb{C}^3$  contains  $\mathcal{D}$ . The line  $L$  in  $\mathbf{G}(2, \mathbb{C}^3)$  through  $T$  and  $T'$  is the set of 2-planes in  $\mathbb{C}^3$  containing the line  $\mathcal{D}$ , so its inverse image under  $\sigma$  is exactly  $\Pi^*$ . Now consider the pencil of lines  $L_t$  through  $T'$ , parameterized so that  $L_0 = L$ . Each  $L_t$  is the set of 2-planes containing some line  $\mathcal{D}_t$ . The family of inverse images of the  $L_t$  which intersect  $U$  is a family  $\{\Pi_{\mathcal{D}_t}^*\}$  of disjoint strict transforms of polar components foliating an open neighborhood of  $\Pi^*$ .

If  $n \geq 3$  we choose an  $(n-3)$ -dimensional subspace  $W \subset \mathbb{C}^n$  transverse to  $T$ . Shrinking  $U$  if necessary, we can assume that  $W$  is transverse to every  $T'' \in U$ . Let  $\mathbf{G}(2, \mathbb{C}^n; W)$  denote the set of 2-planes in  $\mathbb{C}^n$  transverse to  $W$ , so the projection  $p: \mathbb{C}^n \rightarrow \mathbb{C}^n/W$  induces a map  $p': \mathbf{G}(2, \mathbb{C}^n; W) \rightarrow \mathbf{G}(2, \mathbb{C}^n/W) \cong P^2\mathbb{C}$ . We again consider the pencil of lines  $L_t$  in  $\mathbf{G}(2, \mathbb{C}^n/W) \cong P^2\mathbb{C}$  through some point outside  $p'(U)$ . The family of inverse images by  $p' \circ \sigma$  of those of these lines which intersect  $p'(U)$  is again a family of disjoint strict transforms of polar components foliating an open neighborhood of  $\Pi^*$ . The polar corresponding to  $L_t$  is the polar for the projection with kernel  $\mathcal{D}_t$ , where  $\mathcal{D}_t/W \subset \mathbb{C}^n/W$  is again the common line in the family of 2-planes  $L_t \subset \mathbf{G}(2, \mathbb{C}^n/W)$ . Indeed, for any 2-plane  $T'$  in  $\mathbb{C}^n$  transverse to  $W$ , the image  $p(T')$  contains  $\mathcal{D}_t/W$  if and only if  $T'$  intersects  $\mathcal{D}_t$  non-trivially.

Consider now the neighborhood  $\bigcup_{t \in V} \Pi_{\mathcal{D}_t}^*$  of  $\Pi^*$ , where  $V$  is a small closed disk in  $\mathbb{C}$  centered at 0. We denote by  $A^*$  the connected component of  $\bigcup_{t \in V} \Pi_{\mathcal{D}_t}^*$  which contains  $\Pi_0^*$ . Then  $A^* = \bigcup_{t \in V} \Pi_{0, \mathcal{D}_t}^*$ , where  $\Pi_{0, \mathcal{D}_t}$  is a branch of  $\Pi_{\mathcal{D}_t}$ , and  $\Pi_{0, \mathcal{D}_0} = \Pi_0$ . We write  $A := \pi'(A^*) = \bigcup_{t \in V} \Pi_{0, \mathcal{D}_t}$ .

The curves  $\ell(\Pi_{0, \mathcal{D}_t})$  for  $t \in V$  have Puiseux expansions

$$y = \sum_{j \geq 1} a_j(t) x^{pj} \in \mathbb{C}\{x^{1/N}\},$$

where  $a_j(t) \in \mathbb{C}\{\{t\}\}$ . The contact exponent  $s$  is the first  $p_j$  for which the coefficient  $a_j(t)$  is non-constant. Part (1) of the proposition then follows.

*Remark.* In fact, according to the proof of Lemme 1.2.2 (ii) in Teissier [45, p. 462], the family of plane curves  $\ell_{\mathcal{D}}(\Pi_{\mathcal{D}'})$  parameterized by  $(\mathcal{D}, \mathcal{D}') \in \Omega \times \Omega$  is equisingular on a Zariski open neighborhood of the diagonal (a more explicit proof for hypersurfaces is found in Briançon–Henry [7, Theorem 3.7]). It follows that we can choose  $V$  so that the curves  $\ell(\Pi_{0, \mathcal{D}_t})$  for  $t \in V$  form an equisingular family of plane curves.

To prove part (2), we first choose coordinates  $(z_1, \dots, z_n)$  in  $\mathbb{C}^n$  and  $(x, y)$  in  $\mathbb{C}^2$  so that  $\ell$  is the projection  $(x, y) = (z_1, z_2)$ . We may assume that  $z_1$  and  $z_2$  are generic linear forms for  $X$ . The multiplicity of  $z_1$  along the exceptional curve  $E$  is  $N$ . Let  $(u, v)$  be local coordinates centered at  $\Pi_{0, \mathcal{D}_0}^* \cap E$  such that  $v = t$  is the local equation for  $\Pi_{0, \mathcal{D}_t}^*$  and  $z_1 = u^N$ . Then  $z_2$  has the form

$$z_2 = u^N f_0(u) + u^{Ns} \sum_{i \geq 1} v^i f_i(u),$$

where  $f_k(u) \in \mathbb{C}\{\{u\}\}$  for  $k \geq 1$  (and  $u^N f_0(u) = \sum_{j \geq 1} a_j(0) u^{Np_j}$  in our earlier notation).

Now,  $\ell \circ \pi$  has  $\Pi_{0, \mathcal{D}_0}^* \cup \{(u, v) : u = 0\}$  as critical locus. The Jacobian of  $\ell \circ \pi$  is

$$J(\ell \circ \pi)(u, v) = \begin{pmatrix} Nu^{N-1} & 0 \\ \star & u^{Ns}(f_1(u) + 2vf_2(u) + \dots) \end{pmatrix},$$

so  $\Pi_{0, \mathcal{D}_0}^* \cup \{(u, v) : u = 0\}$  has equation

$$Nu^{N+Ns-1}g(u, v) = 0,$$

where  $g(u, v) = f_1(u) + 2vf_2(u) + \dots$ . As  $v = 0$  is the equation of  $\Pi_{0, \mathcal{D}_0}^*$  this implies that  $f_1(u) = 0$  and  $f_2(0) \neq 0$ . So  $g(u, v) = vh_2(u, v)$ , with  $h_2(u, v) = 2f_2(u) + 3vf_3(u) + \dots$  being a unit in  $\mathbb{C}\{\{u, v\}\}$ . Summarizing,

$$\begin{aligned} z_1 &= u^N, \\ z_2 &= u^N f_{2,0}(u) + v^2 u^{Ns} h_2(u, v), \\ z_j &= u^N f_{j,0}(u) + v u^{Ns} h_j(u, v), \quad j \geq 3, \end{aligned}$$

with  $h_2(u, v)$  being a unit. Moreover, at least one  $h_j(u, v)$  with  $j \geq 3$  is a unit by a small adaptation of the argument of [45, p. 464, lines 7 ff.].

The strict transform of  $A_0$  by the resolution  $\pi'$  is the set expressed in local coordinates by

$$A_0^* = \left\{ (u, v) : \left| z_2(u, v) - \sum_{j \geq 1} a_j(0) u^{p_j N} \right| \leq \alpha |z_1(u, v)|^s \right\}.$$

Using the equations for  $z_1$  and  $z_2$  above, we then obtain that

$$A_0^* = \{(u, v) : |v^2 h_2(u, v)| \leq \alpha\}.$$

Since  $h_2$  is a unit in  $\mathbb{C}\{u, v\}$ , the germ  $(A_0, 0)$  agrees up to order  $> s$  with the germ  $(A'_0, 0)$ , where  $A'_0 = \pi'(\{(u, v) : |v|^2 \leq \beta\})$  and  $\beta = \alpha/|h_2(0, 0)|$ . Therefore the germs  $(A_0, 0)$  and  $(A'_0, 0)$  are bilipschitz equivalent, so it suffices to prove part (2) for the germ  $(A'_0, 0)$ . The cone structure of part (2) of the proposition is given by the foliation by solid tori

$$nT_r := \{(u, v) : |z_1(u, v)| = r\} \cap A'_0.$$

Fixing  $c$  such that  $|c|=r$ , the intersection

$$\{(u, v) : z_1(u, v) = c\} \cap A'_0$$

consists of  $N$  meridional disks. Each is to high order of the form

$$\{|c|^s(0, v^2 h_2(0, 0), v h_3(0, 0), \dots, v h_n(0, 0)) : |v| \leq \sqrt{\beta}\},$$

and is therefore bilipschitz equivalent to a flat disk of radius proportional to  $|c|^s$ .

The tangent cone of  $(A'_0, 0)$  is the line  $L$  spanned by  $(1, f_{2,0}(0), f_{3,0}(0), \dots, f_{n,0}(0))$ , which is transverse to the hyperplanes  $z_1=c$ , so the angle between this line  $L$  and the meridional disk sections is bounded away from 0. Let  $D_\varepsilon$  be the disk of radius  $\varepsilon$  in  $L$ . Then, up to bilipschitz equivalence, the transverse disks can be considered to be orthogonal to  $D_\varepsilon$ , giving a metric on  $(A'_0, 0)$  outside the origin as a disk bundle over  $D_\varepsilon \setminus \{0\}$  with fibers orthogonal to this disk and of radius proportional to  $r^s$  at distance  $r$  from the origin. □

*Remark.* (The “very thin zone lemma”) Recall that a Puiseux exponent  $p_j$  of a plane curve given by

$$y = \sum_{i \geq 1} a_i x^{p_i}$$

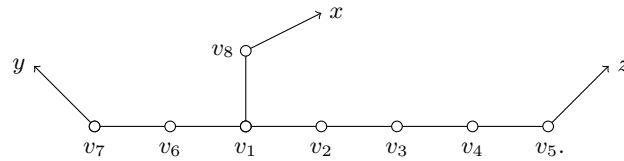
is *characteristic* if the embedded topology of the plane curves

$$y = \sum_{i=1}^{j-1} a_i x^{p_i} \quad \text{and} \quad y = \sum_{i=1}^j a_i x^{p_i}$$

differ; equivalently  $\text{denom}(p_j)$  does not divide  $\text{lcm}_{i < j} \text{denom}(p_i)$ . We denote the characteristic exponents by  $p_{j_k}$  for  $k=1, \dots, r$ , and write  $p_{\max} = p_{j_r}$  for the largest characteristic exponent.

We had believed that the contact exponent of a component of the discriminant curve satisfies  $s \geq p_{\max}$  in general (we called this the “very thin zone lemma”), but the referee pointed out a gap in the proof. And indeed, the “very thin zone lemma” is false. For example, for the hypersurface given by  $(x^2+y^2+z^2)^2+x^5+y^5+z^5=0$ , the components of the polar curve are cusps with exponent  $\frac{3}{2}$  but the contact exponent is 1. The “very thin zone lemma” is true if the multiplicity of  $X$  is  $\leq 3$ , and then  $s$  is often significantly larger than  $p_{\max}$ . In Examples 3.5 and 3.6 below we have respectively  $p_{\max} = \frac{5}{3}$  and  $s = \frac{10}{3}$ , and  $p_{\max} = \frac{17}{9}$  and  $s = \frac{124}{9}$ .

*Example 3.5.* Let  $(X, 0)$  be the  $E_8$  singularity with equation  $x^2+y^3+z^5=0$ . Its resolution graph, with all Euler weights  $-2$  and decorated with arrows corresponding to the strict transforms of the coordinate functions  $x, y$  and  $z$ , is



We denote by  $C_j$  the exceptional curve corresponding to the vertex  $v_j$ . Then the total transform by  $\pi$  of the coordinate functions  $x, y$  and  $z$  are

$$\begin{aligned} (x \circ \pi) &= 15C_1 + 12C_2 + 9C_3 + 6C_4 + 3C_5 + 10C_6 + 5C_7 + 8C_8 + x^*, \\ (y \circ \pi) &= 10C_1 + 8C_2 + 6C_3 + 4C_4 + 2C_5 + 7C_6 + 4C_7 + 5C_8 + y^*, \\ (z \circ \pi) &= 6C_1 + 5C_2 + 4C_3 + 3C_4 + 2C_5 + 4C_6 + 2C_7 + 3C_8 + z^*. \end{aligned}$$

Set  $f(x, y, z) = x^2 + y^3 + z^5$ . The polar curve  $\Pi$  of a generic linear projection

$$\ell: (X, 0) \longrightarrow (\mathbb{C}^2, 0)$$

has equation  $g=0$ , where  $g$  is a generic linear combination of the partial derivatives  $f_x=2x, f_y=3y^2$  and  $f_z=5z^4$ . The multiplicities of  $g$  are given by the minimum of the compact part of the three divisors

$$\begin{aligned} (f_x \circ \pi) &= 15C_1 + 12C_2 + 9C_3 + 6C_4 + 3C_5 + 10C_6 + 5C_7 + 8C_8 + f_x^*, \\ (f_y \circ \pi) &= 20C_1 + 16C_2 + 12C_3 + 8C_4 + 4C_5 + 14C_6 + 8C_7 + 10C_8 + f_y^*, \\ (f_z \circ \pi) &= 24C_1 + 20C_2 + 16C_3 + 12C_4 + 8C_5 + 16C_6 + 8C_7 + 12C_8 + f_z^*. \end{aligned}$$

We then obtain that the total transform of  $g$  is equal to

$$(g \circ \pi) = 15C_1 + 12C_2 + 9C_3 + 6C_4 + 3C_5 + 10C_6 + 5C_7 + 8C_8 + \Pi^*.$$





We now consider again the resolution  $\pi: \tilde{X} \rightarrow X$  defined in §2, which is obtained from a minimal good resolution by first blowing up base points of the linear system of generic hyperplane sections and then blowing up intersection points between  $\mathcal{L}$ -curves. The following results help locate the polar components relative to the Tjurina components of  $\pi$ .

**PROPOSITION 3.7.** *If there are intersecting  $\mathcal{L}$ -curves before the final step then for any generic plane projection, the strict transform of the polar has exactly one component through that common point and it intersects the two  $\mathcal{L}$ -curves transversely.*

*Proof.* Let  $E_\mu$  and  $E_\nu$  denote the two intersecting  $\mathcal{L}$ -curves and choose coordinates  $(u, v)$  centered at the intersection such that  $E_\mu$  and  $E_\nu$  are locally given by  $u=0$  and  $v=0$ , respectively. We assume that our plane projection is given by  $\ell=(x, y): \mathbb{C}^n \rightarrow \mathbb{C}^2$ , so  $x$  and  $y$  are generic linear forms. Then without loss of generality  $x=u^m v^n$  in our local coordinates, and  $y=u^m v^n(a+bu+cv+g(u, v))$  with  $a \neq 0$  and  $g$  of order  $\geq 2$ . The fact that  $E_\mu$  and  $E_\nu$  are  $\mathcal{L}$ -curves means that  $c \neq 0$  and  $b \neq 0$  respectively. The polar component is given by vanishing of the Jacobian determinant

$$\det \frac{\partial(x, y)}{\partial(u, v)} = u^{2m-1} v^{2n-1} (mcv - nbu + mvg_v - nug_u).$$

Modulo terms of order  $\geq 2$ , this vanishing is the equation

$$v = \frac{nb}{mc} u,$$

proving the lemma. □

**LEMMA 3.8.** (Snoussi [42, Théorème 6.9]) *If  $\Gamma_j$  is a Tjurina component of  $\Gamma$  and  $E^{(j)}$  is the union of the  $E_\nu$  with  $\nu \in \Gamma_j$ , then the strict transform of the polar curve of any generic linear projection to  $\mathbb{C}^2$  intersects  $E^{(j)}$ .*

#### 4. Milnor balls

From now on we assume that our coordinates  $(z_1, \dots, z_n)$  in  $\mathbb{C}^n$  chosen so that  $z_1$  and  $z_2$  are generic linear forms and  $\ell := (z_1, z_2): X \rightarrow \mathbb{C}^2$  is a generic linear projection. In this section we denote by  $B_\varepsilon^{2n}$  the standard round ball in  $\mathbb{C}^n$  of radius  $\varepsilon$  and by  $S_\varepsilon^{2n-1}$  its boundary.

The family of Milnor balls we use in the sequel consists of standard “Milnor tubes” associated with the Milnor–Lê fibration for the map  $\zeta := z_1|_X: X \rightarrow \mathbb{C}$ . Namely, for some sufficiently small  $\varepsilon_0$  and some  $R > 0$  we define, for  $\varepsilon \leq \varepsilon_0$ ,

$$B_\varepsilon := \{(z_1, \dots, z_n) : |z_1| \leq \varepsilon \text{ and } |(z_1, \dots, z_n)| \leq R\varepsilon\} \quad \text{and} \quad S_\varepsilon = \partial B_\varepsilon,$$

where  $\varepsilon_0$  and  $R$  are chosen so that, for  $\varepsilon \leq \varepsilon_0$ ,

- (1)  $\zeta^{-1}(t)$  intersects  $S_{R\varepsilon}^{2n-1}$  transversely for  $|t| \leq \varepsilon$ ;
- (2) the polar curves for the projection  $\ell = (z_1, z_2)$  meet  $S_\varepsilon$  in the part  $|z_1| = \varepsilon$ .

PROPOSITION 4.1.  $\varepsilon_0$  and  $R$  as above exist.

*Proof.* We can clearly achieve (2) by choosing  $R$  sufficiently large, since the tangent lines to the polar curve are transverse to the hyperplane  $z_1 = 0$  by genericity of  $z_1$ .

To see that we can achieve (1), note that for  $p \in X$  and  $t = \zeta(p)$  the sphere  $S_{|p|}^{2n-1}$  is not transverse to  $\zeta^{-1}(t)$  at  $p$  if and only if the intersection  $T_p X \cap \{(z_1, \dots, z_n) : z_1 = 0\}$  is orthogonal to the direction  $\vec{p}/|p|$  (considering  $T_p X$  as a subspace of  $\mathbb{C}^n$ ). We will say briefly that condition  $T(p)$  holds.

We must show that there exists  $r > 0$  and  $R > 0$  so that  $T(p)$  fails for all  $p \in X$  with  $R|\zeta(p)| \leq |p| \leq r$ , since then  $R$  and  $\varepsilon_0 := r/R$  do what is required. Suppose the contrary. Then the set

$$S := \{(p, R) \in X \times \mathbb{R}_+ : R|\zeta(p)| \leq |p| \text{ and } T(p) \text{ holds}\}$$

contains points with  $p$  arbitrarily close to 0 and  $R$  arbitrarily large. By the arc selection lemma for semi-algebraic sets, there is an analytic arc

$$\begin{aligned} \gamma: [0, 1] &\longrightarrow X \times \mathbb{R}_+, \\ t &\longmapsto (p(t), R(t)), \end{aligned}$$

with  $\gamma((0, 1]) \subset S$ ,  $\lim_{t \rightarrow 0} p(t) = 0$  and  $\lim_{t \rightarrow 0} R(t) = \infty$ . This arc is then tangent at 0 to a component  $C$  of the curve  $\zeta^{-1}(0)$ . Let  $T$  denote the limit of tangent planes  $T_{p(t)} X$  as  $t \rightarrow 0$ . Then, since the tangent cone to  $\zeta^{-1}(0)$  includes no exceptional directions, we have that  $L' := T \cap \{(z_1, \dots, z_n) : z_1 = 0\} = \lim_{t \rightarrow 0} (T_{p(t)} X \cap \{(z_1, \dots, z_n) : z_1 = 0\})$  is the tangent line to the curve  $C$ . Let  $L$  be the real line tangent to the curve  $p(t)$  at 0. Then  $L$  is in  $T$ , since its direction is a limit of directions  $p(t)/|p(t)|$ , and  $L$  is in  $z_1 = 0$  by the definition of  $\gamma$ . Therefore  $L \subset L'$ , which contradicts that  $T(p)$  holds along the curve  $p(t)$ .  $\square$

## 5. The thin pieces

In this section we prove the thinness of the pieces  $Z_j$  defined in §2. We start with a proof of Proposition 1.3, which states that a semi-algebraic germ  $(Z, 0)$  is contained in a horn neighborhood of its tangent cone.

*Proof.* Without loss of generality,  $Z$  is closed. Consider the function

$$f: \varepsilon \longmapsto \max\{d(x, TZ \cap S_\varepsilon) : x \in Z \cap S_\varepsilon\}.$$

Since  $f$  is semi-algebraic, there exists  $c > 0$  and a Łojasiewicz exponent  $q \geq 1$  such that  $f(\varepsilon) \leq c\varepsilon^q$  for all  $\varepsilon$  sufficiently small. The tangent cone  $TZ$  of  $Z$  is the cone over the Hausdorff limit

$$\lim_{\varepsilon \rightarrow 0} \left( \frac{1}{\varepsilon} Z \cap S_1 \right).$$

Thus, for any  $C > 0$ , the function  $f$  satisfies  $f(\varepsilon) < C\varepsilon$  for  $\varepsilon$  sufficiently small ( $d$  denotes the Hausdorff distance). This implies  $q > 1$  and proves the proposition.  $\square$

PROPOSITION 5.1. (1) For each  $j$ , the tangent cone of  $(Z_j, 0)$  at 0 is an exceptional tangent line  $L_j$  of  $(X, 0)$ .

Let  $q_j > 1$  be such that  $Z_j \cap B_\varepsilon$  is contained in a  $q_j$ -horn neighborhood of the line  $L_j$ .

(2) The restriction  $\zeta_j: Z_j \setminus \{0\} \rightarrow D_\varepsilon^2 \setminus \{0\}$  of  $z_1$  is a locally trivial fibration and there exists  $c_j > 0$  such that each fiber  $\zeta_j^{-1}(t)$  lies in a ball with radius  $c_j t^{q_j}$  centered at the point  $L_j \cap \{(z_1, \dots, z_n): z_1 = t\}$  (we call these fibers the Milnor fibers of  $Z_j$ ).

(3) There is a vector field  $v_j$  on  $Z_j \setminus \{0\}$  which lifts by  $\zeta_j$  the inward radial unit vector field on  $\mathbb{C} \setminus \{0\}$  and has the property that any two integral curves for  $v_j$  starting at points of  $Z_j$  with the same  $z_1$  coordinate approach each other faster than linearly. In particular, the flow along this vector field takes Milnor fibers to Milnor fibers while shrinking them faster than linearly.

Note that it follows from part (1) of this proposition that, with our choice of Milnor balls as in §4, the link  $Z_j^{(\varepsilon)} = Z_j \cap S_\varepsilon$  is included in the  $|z_1| = \varepsilon$  part of  $S_\varepsilon$ .

We need the following lemma. For any  $h$  in the maximal ideal  $\mathfrak{m}_{X,0}$  set

$$\tilde{h} := h \circ \pi: \tilde{X} \rightarrow \mathbb{C}$$

and denote by  $m_\nu(h)$  the multiplicity of  $\tilde{h}$  along the exceptional curve  $E_\nu$ .

LEMMA 5.2. Let  $h_1 = \zeta = z_1|_X$ . For every Tjurina component there exist functions  $h_2, \dots, h_m \in \mathfrak{m}_{X,0}$  such that  $h_1, \dots, h_m$  generate  $\mathfrak{m}_{X,0}$ , and such that for any vertex  $\nu$  of the Tjurina component we have  $m_\nu(h_i) > m_\nu(h_1)$  for  $i > 1$ .

*Proof.* Take any functions  $g_2, \dots, g_m \in \mathfrak{m}_{X,0}$  such that  $h_1, g_2, \dots, g_m$  generate  $\mathfrak{m}_{X,0}$ . Choose a vertex  $\nu$  of the Tjurina component. By the choice of  $z_1$ , we have  $m_\nu(h_1) \leq m_\nu(g_i)$  for all  $i > 1$ . Choose a point  $p$  on  $E_\nu$  distinct from the intersections with other exceptional curves and the strict transform of  $g_i^{-1}(0)$ . Then  $\tilde{h}_1$  and  $\tilde{g}_i$  are given, in local coordinates  $(u, v)$  centered at  $p$ , by

$$\tilde{h}_1 = u^{m_\nu(h_1)}(a_1 + \alpha_1(u, v)) \quad \text{and} \quad \tilde{g}_i = u^{m_\nu(h_1)}(a_i + \alpha_i(u, v)),$$

where  $a_1 \neq 0$  and  $\alpha_1(0, 0) = \alpha_i(0, 0) = 0$ . Let

$$h_i := g_i - \frac{a_i}{a_1} h_1 \quad \text{for } i = 2, \dots, m.$$

Then  $h_1, \dots, h_m$  generate  $\mathfrak{m}_{X,0}$ .

Assume that  $m_\nu(h_i) = m_\nu(h_1)$ . Then the strict transform of  $h_i^{-1}(0)$  passes through  $p$ . Let  $E_{\nu_1}, \dots, E_{\nu_r}$  be the exceptional curves representing the vertices of our Tjurina component  $\Gamma' \subset \Gamma$ , with  $\nu_1 = \nu$ . Let  $I = (E_{\nu_k} \cdot E_{\nu_l})_{1 \leq k, l \leq r}$  be the intersection matrix associated with  $\Gamma'$  and consider the  $r$ -vectors

$$V = {}^t(v_1, \dots, v_r) \quad \text{and} \quad B = {}^t(b_1, \dots, b_r)$$

defined by

$$v_k = m_{\nu_k}(h_i) - m_{\nu_k}(h_1) \quad \text{and} \quad b_k = h_i^* \cdot E_{\nu_k} - h_1^* \cdot E_{\nu_k} + \sum_{\mu \in \mathcal{L}_{\nu_k}} (m_\mu(h_i) - m_\mu(h_1)),$$

where  $\mathcal{L}_{\nu_k}$  denotes the set of  $\mathcal{L}$ -nodes of  $\Gamma$  adjacent to  $\nu_k$ . Since  $h_1^* \cdot E_{\nu_k} = 0$  for all  $k$  and  $h_i^* \cdot E_{\nu_1} \neq 0$ , we have  $b_k \geq 0$  for all  $k$  and  $b_1 > 0$ . Now  $I \cdot V + B = 0$ , so  $V = -I^{-1} \cdot B$ . All entries of  $I^{-1}$  are strictly negative, so all entries of  $V$  are strictly positive, contradicting  $m_\nu(h_i) = m_\nu(h_1)$ . So in fact  $m_\nu(h_i) > m_\nu(h_1)$ .

We now claim that  $m_\mu(h_i) > m_\mu(h_1)$  for  $i > 1$  for any vertex  $\mu$  of the Tjurina component adjacent to  $\nu$  (it then follows inductively for every vertex of the Tjurina component). So let  $\mu$  be such a vertex and assume that  $m_\mu(h_i) = m_\mu(h_1)$ . Consider the meromorphic function  $\tilde{h}_1/\tilde{h}_i$  on  $E_\mu$ . It takes finite values almost everywhere and has a pole at  $E_\mu \cap E_\nu$  so it must have a zero at some point of  $E_\mu$ . This cannot happen since  $m_{\nu'}(h_1) \leq m_{\nu'}(h_i)$  for any  $\nu'$  and the strict transform of the zero set of  $h_1$  only intersects the  $\mathcal{L}$ -nodes ( $h_1$  is the generic linear form).  $\square$

*Proof of Proposition 5.1.* Let  $h_1, \dots, h_m$  be as in Lemma 5.2 and let

$$q_j := \min \left\{ 2, \frac{m_\nu(h_i)}{m_\nu(h_1)} : \nu \in \Gamma_j \text{ and } i > 1 \right\}.$$

For each  $k=2, \dots, n$  one has

$$z_k|_X = \lambda_k h_1 + \beta_k$$

with  $\lambda_k \in \mathbb{C}$  and  $\beta_k \in (h_1^2, h_2, \dots, h_m)$ .

We will prove that the complex line  $L_j \subset \mathbb{C}^n$  parameterized by  $(t, \lambda_2 t, \dots, \lambda_n t)$ ,  $t \in \mathbb{C}$ , is the tangent cone to  $Z_j$ . Since  $Z_j$  contains complex curves (for example the projection  $\pi(\gamma)$  of any curve  $\gamma$  of the exceptional divisor inside  $\mathcal{N}(\Gamma_j)$ ), the tangent cone  $TZ_j$  contains a complex line. Therefore it suffices to prove that  $Z_j \cap B_{\varepsilon_0}$  is contained in a horn neighborhood of  $L_j$ .

Consider local coordinates  $(u, v)$  in a compact neighborhood of a point of

$$E_\nu \setminus \bigcup_{\mu \neq \nu} E_\mu$$

in which  $\tilde{\beta}_i = u^{m_\nu(\beta_i)}(a_i + \alpha_i(u, v))$ , with  $a_i \neq 0$  and  $\alpha_i$  holomorphic. In this neighborhood,

$$|\tilde{z}_i - \lambda_i \tilde{z}_1| = O(|\tilde{z}_1|^{m_\nu(\beta_i)/m_\nu(h_1)}) = O(|\tilde{z}_1|^{q_j}).$$

In a neighborhood of a point  $E_\nu \cap E_\mu$  of intersection of two exceptional curves of the Tjurina component we have local coordinates  $u$  and  $v$  such that  $\tilde{h}_1 = u^{m_\mu(h_1)}v^{m_\nu(h_1)}$  and  $\tilde{\beta}_i = u^{m_\mu(\beta_i)}v^{m_\nu(\beta_i)}(a_i + \alpha_i(u, v))$ , with  $a_i \neq 0$  and  $\alpha_i$  holomorphic. In this neighborhood, we again have  $|\tilde{z}_i - \lambda_i \tilde{z}_1| = O(|\tilde{z}_1|^{q_j})$ .

By compactness of  $\mathcal{N}(\Gamma_j)$ , the estimate  $|\tilde{z}_i - \lambda_i \tilde{z}_1| = O(|\tilde{z}_1|^{q_j})$  holds on all of  $\mathcal{N}(\Gamma_j)$ . Thus, if we define  $f_j: Z_j = \pi(\mathcal{N}(\Gamma_j)) \rightarrow \mathbb{C}^n$  by  $f_j(p) := z_1(p)(1, \lambda_2, \dots, \lambda_n)$ , we have shown that  $|p - f_j(p)| = O(z_1(p)^{q_j})$ . In particular, for  $p \in \mathcal{N}(\Gamma_j)$  the distance of  $\pi(p)$  from 0 is  $O(|z_1(p)|)$ , and therefore  $Z_j \cap B_\epsilon$  is contained in a  $c_j \epsilon^{q_j}$ -neighborhood of the line  $L_j$  for some  $c_j > 0$ .

In particular, we see that  $Z_j$  is thin, and tangent to the line  $L_j$ . Thus each limit of tangent hyperplanes at a sequence of points converging to 0 in  $Z_j \setminus \{0\}$  contains  $L_j$ . We will show that there exist infinitely many such limits, which, by definition, means that  $L_j$  is an exceptional tangent line (this is one of the two implications of [42, Proposition 6.3], see also [23, Proposition 2.2.1], but we did not find a clear statement in the literature). Indeed, for any generic  $(n-2)$ -plane  $H$  let  $\ell_H: \mathbb{C}^n \rightarrow \mathbb{C}^2$  be the projection with kernel  $H$ . By Lemma 3.8 the strict transform  $\Pi^*$  of the polar  $\Pi$  of  $\ell_H|_X$  intersects  $\bigcup_{\nu \in \Gamma_j} E_\nu$ . Let  $C$  be a branch of  $\Pi^*$  which intersects  $\bigcup_{\nu \in \Gamma_j} E_\nu$ . Then, at each  $p \in C$ , the tangent plane to  $X$  at  $p$  intersects  $H$  non-trivially, so the limit of these planes as  $p \rightarrow 0$  in  $C$  is a plane containing  $L_j$  which intersects  $H$  non-trivially. By varying  $H$ , we see that there are infinitely many such limits along sequences of points approaching 0 along curves tangent to  $L_j$ , as desired.

Statement (2) of Proposition 5.1 is just the observation that  $\zeta_j$  is the restriction to  $Z_j \setminus \{0\}$  of the Milnor–Lê fibration for  $z_1: X \rightarrow \mathbb{C}$ .

For (3) we will use local coordinates as above to construct the desired vector field locally in  $\pi^{-1}(Z_j \setminus \{0\})$ ; it can then be glued together by a standard partition-of-unity argument. Specifically, in a neighborhood of a point  $p$  of  $E_\nu \setminus \bigcup_{\mu \neq \nu} E_\mu$ , using coordinates  $(u, v) = (r_u e^{i\theta_u}, r_v e^{i\theta_v})$  with  $\tilde{h}_1 = u^{m_\nu(h_1)}$ , the vector field

$$\left( \frac{1}{m r_u^{m-1}} \frac{\partial}{\partial r_u}, 0 \right)$$

with  $m = m_\nu(h_1)$  works, while in a neighborhood of a point  $E_\nu \cap E_\mu$ , using coordinates with  $\tilde{h}_1 = u^{m_\nu(h_1)}v^{m_\mu(h_1)}$ , the vector field

$$\left( \frac{1}{m r_u^{m-1} r_v^{m'}} \frac{\partial}{\partial r_u}, \frac{1}{m' r_u^m r_v^{m'-1}} \frac{\partial}{\partial r_v} \right)$$

with  $m = m_\nu(h_1)$  and  $m' = m_\mu(h_1)$  works. □

## 6. The thick pieces

In this section we prove the thickness of the pieces  $Y_i$ ,  $i=1, \dots, r$ , defined in §2. Recall that any such  $Y_i$  has the form  $Y=\pi(N(\Gamma_\nu))$ , where  $\Gamma$  is the dual graph of the resolution defined at the beginning of §2 and  $\Gamma_\nu$  is a subgraph consisting of an  $\mathcal{L}$ -node  $\nu$  of  $\Gamma$  and any attached bamboos.

PROPOSITION 6.1.  $Y=\pi(N(\Gamma_\nu))$  is thick.

*Proof.* We use the minimal resolution  $\pi': \tilde{X}' \rightarrow X$  which factors both through  $\pi$  and through Nash modification. We denote by  $\Gamma'$  its resolution graph and by  $\sigma: \tilde{X}' \rightarrow \tilde{X}$  the map such that  $\pi' = \sigma \circ \pi$ . We then have  $Y = \pi'(N(\Gamma'_\nu))$ , where  $\Gamma'_\nu$  is the subgraph of  $\Gamma'$  which projects on  $\Gamma_\nu$  when blowing-down through  $\sigma$ . In particular, notice that if  $G$  is a maximal connected subgraph in  $\Gamma'_\nu \setminus \nu$ , the link of  $\pi'(\mathcal{N}(G))$  is a solid torus.

The thickness of  $Y$  will follow from Lemma 6.2 below, of which part (2) is the most difficult. The proof of (2) uses the techniques introduced in §12, and will be completed in §13 (see the beginning of the proof of Lemma 13.3).

LEMMA 6.2. For any  $\mathcal{L}$ -node  $\nu$  of  $\Gamma'$  we have that

- (1)  $\pi'(\mathcal{N}(\nu))$  is metrically conical;
- (2)  $\pi(N(G))$  is conical for any maximal connected subgraph  $G$  of  $\Gamma'_\nu \setminus \nu$ ;
- (3)  $\pi(N(E_\nu))$  is thick.

Assume that the lemma holds. The conicalness of the union of the conical piece  $\pi'(\mathcal{N}(\nu))$  with the conical pieces  $\pi'(N(G))$  coming from the maximal subgraphs  $G$  of  $\Gamma'_\nu \setminus \nu$  follows from [47, Corollary 0.2], and part (3) of the lemma then completes the proof that  $Y$  is thick.  $\square$

We now prove parts (1) and (3) of Lemma 6.2. As mentioned above, part (2) will be proved later.

*Proof of part (1) of Lemma 6.2.* As before,  $\ell = (z_1, z_2): B_{\varepsilon_0} \rightarrow (\mathbb{C}^2, 0)$  is a generic linear projection to  $\mathbb{C}^2$  and  $\Pi$  is the polar curve for this projection. From now on, we work only inside of a Milnor ball  $B_{\varepsilon_0}$  as defined in §4 and  $X$  now means  $X \cap B_{\varepsilon_0}$ .

Denote by  $\Delta = \Delta_1 \cup \dots \cup \Delta_k \subset \mathbb{C}^2$  the decomposition of the discriminant curve  $\Delta$  for  $\ell$  into its irreducible components. By genericity, we may assume that the tangent lines in  $\mathbb{C}^2$  to the  $\Delta_i$ 's are of the form  $z_2 = b_i z_1$ . Set

$$V_i := \{(z_1, z_2) \in \mathbb{C}^2 : |z_1| \leq \varepsilon_0 \text{ and } |z_2 - b_i z_1| \leq \eta |z_1|\},$$

where we choose  $\eta$  so small that  $V_i \cap V_j = \{0\}$  if  $b_i \neq b_j$  and  $\varepsilon_0$  so small that

$$\Delta_i \cap \{(z_1, z_2) : |z_1| \leq \varepsilon_0\} \subseteq V_i.$$

Notice that if two  $\Delta_i$ 's are tangent then the corresponding  $V_i$ 's are the same.

Let  $W_{i1}, \dots, W_{ij_i}$  be the closure of the connected components of  $X \cap \ell^{-1}(V_i \setminus \{0\})$  which contain components of the polar curve. Then the restriction of  $\ell$  to  $\overline{X \setminus \bigcup_{ij} W_{ij}}$  is a bilipschitz local homeomorphism by Proposition 3.4. In particular, this set is metrically conical.

Assume that the strict transform by  $\pi'$  of a component  $\Pi_0$  of  $\Pi$  intersects the  $\mathcal{L}$ -node  $E_\nu$ . By definition of  $\pi'$ ,  $p = \Pi_0^* \cap E_\nu$  is a smooth point of the exceptional divisor  $E = (\pi')^{-1}(0)$  and  $p$  is not a base point of the family of polar curves of generic plane projections. So, varying the plane projection varies locally the intersection point of  $E_\nu$  with the strict transform of the polar component, and hence also the tangent line of  $\Pi_0$ . We call  $\Pi_0$  a *moving polar component*. The contact exponent of this moving polar component is  $s=1$ , so we can take the corresponding  $W_{ij}$  containing  $\Pi_0$  to be the set  $A_0$  of Proposition 3.4 (2) and it follows that  $W_{ij}$  is metrically conical. Hence, if  $W$  denotes the union of  $W_{ij}$  such that  $\Pi \cap W_{ij}$  is not a moving polar component, the semi-algebraic set  $\overline{X \setminus W}$  is metrically conical. Since the coordinates at the double points of  $E$  on an  $\mathcal{L}$ -curve  $E_\nu$  can be chosen so that  $\mathcal{N}(\nu)$  is a connected component of  $\pi^{-1}(\overline{X \setminus W})$ , part (1) of the lemma is proved.  $\square$

*Proof of part (3) of Lemma 6.2.* Let  $\mu$  be an adjacent vertex to our  $\mathcal{L}$ -node  $\nu$ . We must show that the structure just proved to be conical can be extended to a thick structure over  $N(E_\nu) \cap N(E_\mu)$ . Take local coordinates  $u$  and  $v$  at the intersection of  $E_\nu$  and  $E_\mu$  such that  $u=0$  (resp.  $v=0$ ) is a local equation for  $E_\nu$  (resp.  $E_\mu$ ).

By Lemma 5.2, we can choose  $c \in \mathbb{C}$  so that the linear form  $h_2 = z_1 - cz_2$  satisfies  $m_\mu(z_1) < m_\mu(h_2)$ . We change coordinates to replace  $z_2$  by  $h_2$ , which does not change the linear projection  $\ell$ , so we still have that  $m_\nu(z_1) = m_\nu(h_2)$ . So we may assume that in our local coordinates  $z_1 = u^{m_\nu(z_1)} v^{m_\mu(z_1)}$  and  $z_2 = u^{m_\nu(z_1)} v^{m_\mu(h_2)} (a + g(u, v))$ , where  $a \in \mathbb{C}^*$  and  $g(0, 0) = 0$ . To higher order, the lines  $v=c$  for  $c \in \mathbb{C}$  project onto radial lines of the form  $z_2 = c' z_1$ , and the sets  $|u|=d$  with  $d \in \mathbb{R}^+$  project to horn-shaped real hypersurfaces of the form  $|z_2| = d' |z_1|^{m_\mu(h_2)/m_\mu(z_1)}$ . In particular the image of a small domain of the form  $\{(u, v) : |u| \leq d_1 \text{ and } |v| \leq d_2\}$  is thick. See Figure 3 for a schematic real picture. By Proposition 3.3 the local bilipschitz constant remains bounded in this added region, so the desired result again follows by pulling back the standard conical structure from  $\mathbb{C}^2$ .  $\square$

### 7. Fast loops

We recall the definition of a “fast loop” in the sense of [3], which we will here sometimes call “fast loop of the first kind”, since we also define a closely related concept of “fast loop of the second kind”. We first need another definition.

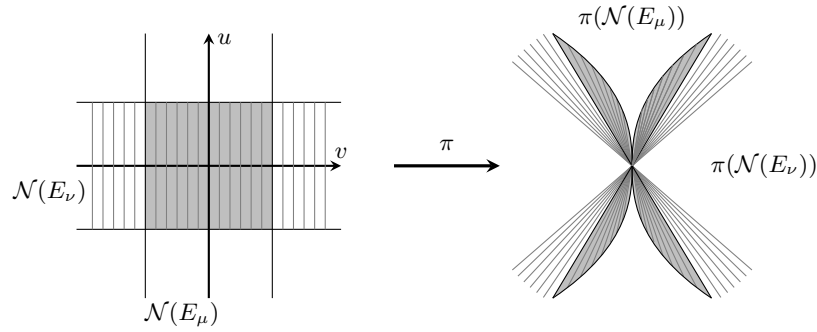


Figure 3. Thickness near the boundary of a thick piece.

*Definition 7.1.* If  $M$  is a compact Riemannian manifold and  $\gamma$  is a closed rectifiable null-homotopic curve in  $M$ , the *isoperimetric ratio* for  $\gamma$  is the infimum of areas of singular disks in  $M$  which  $\gamma$  bounds, divided by the square of the length of  $\gamma$ .

*Definition 7.2.* Let  $\gamma$  be a closed curve in the link  $X^{(\epsilon_0)} = X \cap S_{\epsilon_0}$ . Suppose there exists a continuous family of loops  $\gamma_\epsilon: S^1 \rightarrow X^{(\epsilon)}$ ,  $\epsilon \leq \epsilon_0$ , whose lengths shrink faster than linearly in  $\epsilon$  and with  $\gamma_{\epsilon_0} = \gamma$ . If  $\gamma$  is homotopically non-trivial in  $X^{(\epsilon_0)}$  we call the family  $\{\gamma_\epsilon\}_{0 < \epsilon \leq \epsilon_0}$  a *fast loop of the first kind* or simply a *fast loop*. If  $\gamma$  is homotopically trivial but the isoperimetric ratio of  $\gamma_\epsilon$  tends to  $\infty$  as  $\epsilon \rightarrow 0$  we call the family  $\{\gamma_\epsilon\}_{0 < \epsilon \leq \epsilon_0}$  a *fast loop of the second kind*.<sup>(2)</sup>

**PROPOSITION 7.3.** *The existence of a fast loop of the first or second kind is an obstruction to the metric conicalness of  $(X, 0)$ .*

*Proof.* It is shown [3] that a fast loop of the first kind cannot exist in a metric cone, so its existence is an obstruction to metric conicalness.

For a fixed Riemannian manifold  $M$  the isoperimetric ratio for a given null-homotopic curve is invariant under scaling of the metric and is changed by a factor of at most  $K^4$  by a  $K$ -bilipschitz homeomorphism of  $M$ . It follows that if  $X$  is metrically conical then for any  $C > 0$  there is an overall bound on the isoperimetric ratio of null-homotopic curves in  $X^{(\epsilon)}$  of length  $\leq C\epsilon$  as  $\epsilon \rightarrow 0$ .  $\square$

**THEOREM 7.4.** *Any curve in a Milnor fiber of a thin zone  $Z_j^{(\epsilon_0)}$  of  $X^{(\epsilon_0)}$  which is homotopically non-trivial in  $Z_j^{(\epsilon_0)}$  gives a fast loop of the first or second kind.*

*Proof.* Using the vector field of Proposition 5.1, any closed curve  $\gamma$  in the Milnor fiber of the link  $Z_j^{(\epsilon_0)}$  of a thin piece  $Z_j$  of  $X^{(\epsilon_0)}$  gives rise to a continuous family of closed

---

<sup>(2)</sup> Fast loops of the second kind were needed in an early version of this paper but not in the current version. We have retained them since their analogs are useful in higher dimension.



curves  $\gamma_\varepsilon: [0, 1] \rightarrow Z_j^{(\varepsilon)}$ ,  $\varepsilon \leq \varepsilon_0$ , whose lengths shrink faster than linearly with respect to  $\varepsilon$ .

If  $\gamma$  is homotopically non-trivial in  $X^{(\varepsilon_0)}$  then  $\{\gamma_\varepsilon\}_{0 < \varepsilon \leq \varepsilon_0}$  is a fast loop of the first kind. Otherwise, let  $f: D_\varepsilon \rightarrow X^{(\varepsilon)}$  be a map of a disk with boundary  $\gamma_\varepsilon$ .

Let  $Y = \bigcup_{i=1}^r Y_i$  denote the thick part of  $X$ . Let  $Y_\varepsilon \subset Y$  for  $\varepsilon \leq \varepsilon_0$  be a collection of conical subsets as in Definition 1.2. The link of  $Y_\varepsilon$  is  $Y^{(\varepsilon)}$ . We can approximate  $f$  by a smooth map transverse to  $\partial Y^{(\varepsilon)}$  while only increasing area by an arbitrarily small factor. Then  $f(D) \cap \partial Y^{(\varepsilon)}$  consists of smooth immersed closed curves. A standard innermost disk argument shows that at least one of them is homotopically non-trivial in  $\partial Y^{(\varepsilon)}$  and bounds a disk  $D'$  in  $Y^{(\varepsilon)}$  obtained by restricting  $f$  to a subdisk of  $D$ . Since there is a lower bound proportional to  $\varepsilon$  on the length of essential closed curves in  $\partial Y^{(\varepsilon)}$  and  $Y$  is thick, the area of  $D'$  is bounded below proportional to  $\varepsilon^2$ . It follows that the isoperimetric ratio for  $\gamma_\varepsilon$  tends to  $\infty$  as  $\varepsilon \rightarrow 0$ . □

**THEOREM 7.5.** (1) *Every thin piece  $Z_j$  contains a fast loop (of the first kind). In fact every boundary component of a Milnor fiber  $F_j$  of  $Z_j$  is a fast loop.*

(2) *Every point  $p \in Z_j$  lies on some fast loop  $\{\gamma_\varepsilon\}_{0 < \varepsilon \leq \varepsilon_0}$  and every real tangent line to  $Z_j$  is tangent to  $\bigcup_\varepsilon \gamma_\varepsilon \cup \{0\}$  for some such fast loop.*

*Proof.* Part (2) follows from part (1) because the link  $Z_j^{(\varepsilon_0)}$  is foliated by Milnor fibers and a boundary component of a Milnor fiber  $\zeta_j^{-1}(t)$  can be isotoped into a loop  $\gamma$  through any point of the same Milnor fiber. The family  $\{\gamma_\varepsilon\}_{0 < \varepsilon \leq \varepsilon_0}$  obtained from  $\gamma$  using the vector field of Proposition 5.1 is a fast loop whose tangent line is the real line  $L_j \cap \{(z_1, \dots, z_n) : \arg z_1 = \arg t\}$ .

We will actually prove a stronger result than part (1) of the theorem, since it is needed in §14. First we need a remark.

*Remark 7.6.* The monodromy map  $\phi_j: F_j \rightarrow F_j$  for the fibration  $\zeta_j|_{Z_j^{(\varepsilon_0)}}$  is a quasi-periodic map, so after an isotopy it has a decomposition into subsurfaces  $F_\nu$  on which  $\phi_j$  has finite order acting with connected quotient, connected by families of annuli which  $\phi_j$  cyclically permutes by a generalized Dehn twist (i.e., some power is a Dehn twist on each annulus of the family). The minimal such decomposition is the Thurston–Nielsen decomposition, which is unique up to isotopy. By [39, Lemme 4.4] each  $F_\nu$  is associated with a node  $\nu$  of  $\Gamma_j$  while each string joining two nodes  $\nu$  and  $\nu'$  of  $\Gamma_j$  corresponds to a  $\phi_j$ -orbit of annuli connecting  $F_\nu$  to  $F_{\nu'}$ . This decomposition of the fiber  $F_j$  corresponds to the minimal decomposition of  $Z_j^{(\varepsilon_0)}$  into Seifert fibered manifolds  $Z_\nu^{(\varepsilon_0)}$ , with thickened tori between them, i.e., the JSJ decomposition.

The following proposition is more general than part (1) of Theorem 7.5, and therefore completes its proof. □

PROPOSITION 7.7. *Each boundary component of an  $F_\nu$  gives a fast loop (of the first kind).*

*Proof.* We assume the contrary, that some boundary component  $\gamma$  of  $F_\nu$  is homotopically trivial in  $X^{(\varepsilon_0)}$ . We will derive a contradiction.

Let  $T$  be the component of  $\partial Z_\nu^{(\varepsilon_0)}$  which contains  $\gamma$ . Then it is compressible, so it contains an essential closed curve which bounds a disk to one side of  $T$  or the other. Cutting  $X^{(\varepsilon_0)}$  along  $T$  gives a manifold with a compressible boundary torus. But a plumbed manifold-with-boundary given by negative definite plumbing has a compressible boundary component if and only if it is a solid torus, see [33] and [28]. So  $T$  separates  $X^{(\varepsilon_0)}$  into two pieces, one of which is a solid torus. Call it  $A$ .

LEMMA 7.8.  *$\gamma$  represents a non-trivial element of  $\pi_1(A)$ .*

*Proof.* Let  $\Gamma_0$  be the subgraph of  $\Gamma$  representing  $A$ , i.e., a component of the subgraph of  $\Gamma$  obtained by removing the edge corresponding to  $T$ . We will attach an arrow to  $\Gamma_0$  where that edge was. Then the marked graph  $\Gamma_0$  is the plumbing graph for the solid torus  $A$ . We note that  $\Gamma_0$  must contain at least one  $\mathcal{L}$ -node, since otherwise  $A$  would have to be  $Z_j^{(\varepsilon_0)}$  or a union of pieces of its JSJ decomposition, but this cannot be a solid torus.

We now blow down  $\Gamma_0$  to eliminate all  $(-1)$ -curves. We then obtain a bamboo  $\Gamma'$  with negative definite matrix and an arrow at one extremity. It is the resolution graph of some cyclic quotient singularity  $Q = \mathbb{C}^2/(\mathbb{Z}/p)$  and from this point of view the arrow represents the strict transform of the zero set of the function  $x^p$  on  $Q$ , where  $x$  and  $y$  are the coordinates of  $\mathbb{C}^2$ . The Milnor fibers of this function give the meridian disks of the solid torus  $A$ . Let  $D$  be such a meridian disk. In the resolution, the intersection of  $D$  with any curvette (transverse complex disk to an exceptional curve) is positive (namely an entry of the first row of  $pS_{\Gamma'}^{-1}$ , where  $S_{\Gamma'}$  is the intersection matrix associated with  $\Gamma'$ ). Since  $\Gamma_0$  contains an  $\mathcal{L}$ -node, then in particular  $D$  intersects transversely the strict transform  $z_1^*$  of  $z_1$  and we set  $D \cdot z_1^* = s > 0$ .

Let us go back to our initial  $X^{(\varepsilon_0)}$ . Recall that in this paper we use the Milnor balls  $B_\varepsilon$  which are standard Milnor tubes for the Milnor–Lê fibration  $\zeta = z_1|_X$  (see §4). Denote again by  $\zeta: T \rightarrow S_{\varepsilon_0}^1$  the restriction of  $z_1$  to  $T = z_1^{-1}(S_{\varepsilon_0}^1) \cap X^{(\varepsilon_0)}$ , and let  $\zeta_*: H_1(T; \mathbb{Z}) \rightarrow \mathbb{Z}$  be the induced map.

The meridian curve  $c = \partial D$  of  $A$  is homologically equivalent to the sum of the boundary curves  $c_1, \dots, c_s$  of small disk neighborhoods of the intersection points of  $D$  with  $z_1^*$ . The Milnor–Lê fibration  $\zeta$  is equivalent to the Milnor fibration

$$z_1/|z_1|: X^{(\varepsilon_0)} \setminus L \longrightarrow \mathbb{S}^1$$

outside a neighborhood of the link

$$L = \{(z_1, \dots, z_n) : z_1 = 0\} \cap X^{(\varepsilon_0)},$$

and the latter is an open-book fibration with binding  $L$ . Therefore  $\zeta_*(c_i)=1$  for each  $i=1, \dots, s$  and  $\zeta_*(c)=s>0$ . Since  $\zeta_*(\gamma)=0$ , this implies the lemma.  $\square$

We now know that  $\gamma$  is represented by a non-zero multiple of the core of the solid torus  $A$ . This core curve is the curvette boundary for the curvette transverse to the end curve of the bamboo obtained by blowing down  $\Gamma_0$  in the above proof.

LEMMA 7.9. *Given any good resolution graph (not necessarily minimal) for a normal complex surface singularity whose link  $\Sigma$  has infinite fundamental group, the boundary of a curvette always represents an element of infinite order in  $\pi_1(\Sigma)$ .*

*Proof.* After blowing down to obtain a minimal good resolution graph, the only case to check is when the blown down curvette  $c$  intersects a bamboo, since otherwise its boundary represents a non-trivial element of the fundamental group of some piece of the JSJ decomposition of  $\Sigma$  and each such piece embeds  $\pi_1$ -injectively into  $\Sigma$ . If  $c$  intersects a single exceptional curve  $E_1$  of the bamboo, then its boundary is homotopic to a positive multiple of the curvette boundary for  $E_1$ , so by the argument in the proof of the previous lemma, the boundary of  $c$  is homotopic to a positive multiple of the core curve of the corresponding solid torus. As a fiber of the Seifert fibered structure on a JSJ component of  $\Sigma$ , this element has infinite order in  $\pi_1$  of the component and therefore of  $\Sigma$ . Finally, suppose that  $c$  intersects the intersection point of two exceptional divisors  $E_1$  and  $E_2$  of the bamboo. Then, in local coordinates  $(u, v)$  with  $E_1 = \{(u, v) : u = 0\}$  and  $E_2 = \{(u, v) : v = 0\}$ , the curvette can be given by a Puiseux expansion  $u = \sum_i v^{q_i/p_i}$ , where, without loss of generality,  $q_i > p_i$ . Then the boundary of  $c$  is an iterated torus knot in this coordinate system which homologically is a positive multiple of  $p_1\mu_1 + q_1\mu_2$ , where  $\mu_i$  is a curvette boundary of  $E_i$  for  $i=1, 2$ . We conclude by applying the previous argument to  $\mu_1$  and  $\mu_2$  that  $c$  is a positive multiple of the core curve of the solid torus, completing the proof.  $\square$

Returning to the proof of Proposition 7.7, we see that if  $\pi_1(X^{(\varepsilon_0)})$  is infinite then the curve  $\gamma$  of Lemma 7.8 is non-trivial in  $\pi_1(X^{(\varepsilon_0)})$  by Lemma 7.9, proving the proposition in this case.

It remains to prove the proposition when  $\pi_1(X^{(\varepsilon_0)})$  is finite. Then  $(X, 0)$  is a rational singularity ([6], [15]), and the link of  $X^{(\varepsilon_0)}$  is either a lens space or a Seifert manifold with three exceptional fibers with multiplicities  $(\alpha_1, \alpha_2, \alpha_3)$  equal to  $(2, 3, 3)$ ,  $(2, 3, 4)$ ,  $(2, 3, 5)$  or  $(2, 2, k)$  with  $k \geq 2$ .

We will use the following lemma.

LEMMA 7.10. *Let  $A$  and  $\gamma$  as in Lemma 7.8. Suppose that the subgraph  $\Gamma_0$  of  $\Gamma$  representing the solid torus  $A$  is a bamboo*

$$\begin{array}{ccc} -b_1 & -b_2 & \dots & -b_r \\ \circ & \text{---} & \circ & \text{---} & \dots & \text{---} & \circ \\ \nu_1 & \nu_2 & & & & & \nu_r \end{array}$$

attached at vertex  $\nu_1$  to the vertex  $\nu$  of  $\Gamma$ . Denote by  $m_\nu$  and  $m_{\nu_1}$  the multiplicities of the function  $\tilde{z}_1 = z_1 \circ \pi$  along  $E_\nu$  and  $E_{\nu_1}$ , and let  $(\alpha, \beta)$  be the Seifert invariant of the core of  $A$  viewed as a singular fiber of the  $S^1$ -fibration over  $E_\nu$ , i.e.,  $\alpha/\beta = [b_{\nu_1}, \dots, b_{\nu_n}]$ . Let  $C$  be the core of  $A$  oriented as the boundary of a curvette of  $E_{\nu_r}$ . Then, with  $d = \text{gcd}(m_\nu, m_{\nu_1})$ , we have

$$\gamma = \left( \frac{m_{\nu_1}}{d} \alpha - \frac{m_\nu}{d} \beta \right) C \quad \text{in } H_1(A; \mathbb{Z}).$$

*Proof.* Orient the torus  $T$  as a boundary component of  $A$ . Let  $C_\nu$  and  $C_{\nu_1}$  in  $T$  be boundaries of curvettes of  $E_\nu$  and  $E_{\nu_1}$ . Then

$$\gamma = \frac{m_\nu}{d} C_{\nu_1} - \frac{m_{\nu_1}}{d} C_\nu,$$

and the meridian of  $A$  on  $T$  is given by  $M = \alpha C_{\nu_1} + \beta C_\nu$ . Then  $\gamma = \lambda C$  where  $\lambda = M \cdot \gamma$ . As  $C_{\nu_1} \cdot C_\nu = +1$  on  $T$ , we then obtain the stated formula.  $\square$

Let us return to the proof of Proposition 7.7. When  $X^{(\varepsilon_0)}$  is a lens space, then the minimal resolution graph is a bamboo

$$\begin{array}{ccc} -b_1 & -b_2 & \dots & -b_n \\ \circ & \text{---} & \circ & \text{---} & \dots & \text{---} & \circ \end{array}$$

The function  $\tilde{z}_1$  has multiplicity 1 along each  $E_i$ , and the strict transform of  $z_1$  has  $b_1 - 1$  components intersecting  $E_1$ ,  $b_n - 1$  components on  $E_n$ , and  $b_i - 2$  components on any other curve  $E_i$ . In particular the  $\mathcal{L}$ -nodes are the two extremal vertices of the bamboo and any vertex with  $b_i \geq 3$ . To get the adapted resolution graph of §2 we should blow up once between any two adjacent  $\mathcal{L}$ -nodes. Then the subgraph  $\Gamma_j$  associated with our thin piece  $Z_j$  is either a  $(-1)$ -weighted vertex or a maximal string  $\nu_i, \nu_{i+1}, \dots, \nu_k$  of vertices excluding  $\nu_1$  and  $\nu_n$  carrying self-intersections  $b_j = -2$ .

We first consider the second case. Let  $\gamma$  be the intersection of the Milnor fiber of  $Z_j$  with the plumbing torus at the intersection of  $E_k$  and  $E_{k+1}$ . According to Lemma 7.10, we have  $\gamma = (\alpha - \beta)C$ , where  $C$  is the boundary of a curvette of  $E_n$  and

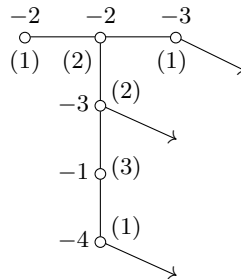
$$\frac{\alpha}{\beta} = [b_{k+1}, \dots, b_n]$$

with  $E_i^2 = -b_i$ . But  $C$  is a generator of the cyclic group  $\pi_1(X^{(\varepsilon_0)})$ , which has order  $p = [b_1, \dots, b_n]$ . Since  $0 < \alpha - \beta \leq \alpha < p$ , we obtain that  $\gamma$  is non-trivial in  $\pi_1(X^{(\varepsilon_0)})$ .

For the case of a  $(-1)$ -vertex we can work in the minimal resolution with the two adjacent  $\mathcal{L}$ -curves  $E_k$  and  $E_{k+1}$  and the plumbing torus  $T$  at their intersection, since blowing down the  $(-1)$ -curve does not change  $\gamma$ . So it is the same calculation as before. This completes the lens space case.

We now assume that  $X^{(\varepsilon_0)}$  has 3 exceptional fibers whose multiplicities  $(\alpha_1, \alpha_2, \alpha_3)$  are  $(2, 3, 3)$ ,  $(2, 3, 4)$ ,  $(2, 3, 5)$  or  $(2, 2, k)$  with  $k \geq 2$ . Then the graph  $\Gamma$  is star-shaped with three branches and with a central node whose Euler number is  $e \leq -2$ . If  $e \leq -3$ , then  $\tilde{z}_1$  has multiplicity 1 on each exceptional curve and we conclude using Lemma 7.10 as in the lens space case.

When  $e = -2$ , the multiplicities of  $\tilde{z}_1$  are not all equal to 1, and we have to examine all the cases one by one. For  $(\alpha_1, \alpha_2, \alpha_3) = (2, 3, 5)$ , there are eight possible values for the Seifert pairs, which are  $(2, 1)$ ,  $(3, \beta_2)$  and  $(5, \beta_3)$ , where  $\beta_2 \in \{1, 2\}$  and  $\beta_3 \in \{1, 2, 3, 4\}$ . For example, in the case  $\beta_2 = 1$  and  $\beta_3 = 3$  the resolution graph  $\Gamma$  is represented by



The arrows represent the strict transform of the generic linear function  $z_1$ . There are two thin zones obtained by deleting the vertices with arrows and their adjacent edges, leading to four curves  $\gamma$  to be checked. Lemma 7.10 computes them as  $C_3$ ,  $2C_5$ ,  $C_5$  and  $C_5$ , respectively, where  $C_p$  is the exceptional fiber of degree  $p$ . The other cases are easily checked in the same way. The case  $(2, 2, k)$  gives an infinite family similar to the lens space case. □

Proposition 7.3 and either one of Theorems 7.4 and 7.5 show the following result.

**COROLLARY 7.11.**  *$(X, 0)$  is metrically conical if and only if there are no thin pieces. Equivalently,  $\Gamma$  has only one node, and it is the unique  $\mathcal{L}$ -node.*

*Example 7.12.* Let  $(X, 0) \subset (\mathbb{C}^3, 0)$ , defined by  $x^a + y^b + z^b = 0$  with  $1 \leq a < b$ . Then the graph  $\Gamma$  is star-shaped with  $b$  bamboos and the single  $\mathcal{L}$ -node is the central vertex. Therefore,  $(X, 0)$  is metrically conical. This metric conicalness was first proved in [4]. The rational singularities which are metrically conical have been determined by Pedersen [37]; they form an interesting three-discrete-parameter family.

### 8. Existence and uniqueness of the minimal thick-thin decomposition

We first prove the existence.

LEMMA 8.1. *The thick-thin decomposition constructed in §2 is minimal, as defined in Definition 1.5.*

*Proof.* Any real tangent line to  $Z_j$  is a tangent line to some fast loop  $\{\gamma_\varepsilon\}_{0 < \varepsilon \leq \varepsilon_0}$  by Theorem 7.5. For any other thick-thin decomposition this fast loop is outside any conical part of the thick part for all sufficiently small  $\varepsilon$ , so its tangent line is a tangent line to a thin part. It follows that this thick-thin decomposition contains a thin piece which is tangent to the tangent cone of  $Z_j$ . Thus the first condition of minimality is satisfied. For the second condition, note that, according to the proof of Proposition 6.1,  $\bigcup_{j=1}^s N(\Gamma_j)$  has conical complement and that the  $N(\Gamma_j)$ 's are pairwise disjoint except at the origin and each contains its respective  $Z_j$ . Consider some thick-thin decomposition of  $(X, 0)$  with thin pieces  $Z'_i$ ,  $i=1, \dots, s'$ . Each  $N(\Gamma_j)$  must have a  $Z'_i$  in it since each  $N(\Gamma_j)$  contains fast loops, and this  $Z'_i$  is completely inside  $N(\Gamma_j)$  (as a germ at 0), as its tangent space is contained in the tangent line to  $Z_j$ . Thus  $s \leq s'$ .  $\square$

We restate the uniqueness theorem of the introduction.

THEOREM. (Uniqueness part of Theorem 1.6) *For any two minimal thick-thin decompositions of  $(X, 0)$  there exists  $q > 1$  and a homeomorphism of the germ  $(X, 0)$  to itself which takes one decomposition to the other and moves each  $x \in X$  a distance at most  $|x|^q$ .*

*Proof.* It follows from the proof of Lemma 8.1 that any two minimal thick-thin decompositions have the same numbers of thick and thin pieces. Let us consider the thick-thin decomposition

$$(X, 0) = \bigcup_{i=1}^r (Y_i, 0) \cup \bigcup_{j=1}^s (Z_j, 0)$$

constructed in §2, and another minimal thick-thin decomposition

$$(X, 0) = \bigcup_{i=1}^r (Y'_i, 0) \cup \bigcup_{j=1}^s (Z'_j, 0).$$

They can be indexed so that for each  $j$  the intersection  $Z_j \cap Z'_j \cap (B_\varepsilon \setminus \{0\})$  is non-empty for all small  $\varepsilon$ . (This is not hard to see, but in fact we only need that  $Z_j$  and  $Z'_j$  are very close to each other in the sense that the distance between  $Z_j \cap S_\varepsilon$  and  $Z'_j \cap S_\varepsilon$  is bounded by  $c\varepsilon^{q'}$  for some  $c > 0$  and  $q' > 1$ , which is immediate from the proof of Lemma 8.1.)

Definition 1.2 says that  $Y = \bigcup_{i=1}^r Y_i$  is the union of metrically conical subsets  $Y_\varepsilon \subset B_\varepsilon$ ,  $0 < \varepsilon \leq \varepsilon_0$ . We will denote by  $\partial_0 Y_\varepsilon := \overline{\partial Y_\varepsilon} \setminus (Y_\varepsilon \cap S_\varepsilon)$ , the “sides” of these cones, which form a disjoint union of cones on tori. We do the same for  $Y' = \bigcup_{i=1}^r Y'_i$ .

The limit as  $\varepsilon \rightarrow 0$  of the tangent cones of any component of  $\partial_0 Y_\varepsilon$  is the tangent line to a  $Z_j$ . It follows that for all  $\varepsilon_1$  sufficiently small  $\partial_0 Y'_{\varepsilon_1}$  will be “outside”  $\partial_0 Y_{\varepsilon_0}$  in the sense that it is disjoint from  $Y_{\varepsilon_0}$  except at 0. Choose  $\varepsilon_1 \leq \varepsilon_0$  so that this is the case. Similarly, choose  $0 < \varepsilon_3 \leq \varepsilon_2 \leq \varepsilon_1$  so that  $\partial_0 Y_{\varepsilon_2}$  is outside  $\partial_0 Y'_{\varepsilon_1}$  and  $\partial_0 Y'_{\varepsilon_3}$  is outside  $\partial_0 Y_{\varepsilon_2}$ .

Now consider the 3-manifold  $M \subset S_{\varepsilon_3}$  consisting of what is between  $\partial_0 Y_{\varepsilon_0}$  and  $\partial_0 Y'_{\varepsilon_3}$  in  $X \cap S_{\varepsilon_3}$ . We can write  $M$  as  $M_1 \cup M_2 \cup M_3$ , where  $M_1$  is between  $\partial_0 Y_{\varepsilon_0}$  and  $\partial_0 Y'_{\varepsilon_1}$ ,  $M_2$  is between  $\partial_0 Y'_{\varepsilon_1}$  and  $\partial_0 Y_{\varepsilon_2}$  and  $M_3$  is between  $\partial_0 Y_{\varepsilon_2}$  and  $\partial_0 Y'_{\varepsilon_3}$ . Each component of  $M_1 \cup M_2$  is homeomorphic to  $\partial_1 M_2 \times I$  and each component of  $M_2 \cup M_3$  is homeomorphic to  $\partial_0 M_2 \times I$ , so it follows by a standard argument that each component of  $M_2$  is homeomorphic to  $\partial_0 M_2 \times I$ . ( $M_2$  is an invertible bordism between its boundaries and apply Stallings’s  $h$ -cobordism theorem [44]; alternatively, use Waldhausen’s classification of incompressible surfaces in surface  $\times I$  in [48].)

Set  $Z = \bigcup_{j=1}^s Z_j$  and  $Z' = \bigcup_{j=1}^s Z'_j$ . The complement of the  $\varepsilon_3$ -link of  $Y_{\varepsilon_2}$  in  $X^{(\varepsilon_3)}$  is the union of  $Z^{(\varepsilon_3)}$  and a collar neighborhood of its boundary and is hence isotopic to  $Z^{(\varepsilon_3)}$ . It is also isotopic to its union with  $M_2$ , which is the complement of the  $\varepsilon_3$ -link of  $Y'_{\varepsilon_1}$ . This latter is the union of  $(Z')^{(\varepsilon_3)}$  and a collar, and is hence isotopic to  $(Z')^{(\varepsilon_3)}$ . Thus the links of  $Z$  and  $Z'$  are homeomorphic, so  $Z$  and  $Z'$  are homeomorphic, and we can choose this homeomorphism to move any point  $x$  a distance at most  $|x|^q$  for any  $q < q'$ , where  $q'$  is defined above. □

We can also characterize, as in the following theorem, the unique minimal thick-thin decomposition in terms of the analogy with the Margulis thick-thin decomposition mentioned in the introduction. The proof is immediate from the proof of Lemma 8.1.

**THEOREM 8.2.** *The canonical thick-thin decomposition can be characterized among thick-thin decompositions by the following condition: For any sufficiently small  $q > 1$  there exists  $\varepsilon_0 > 0$  such that for all  $\varepsilon \leq \varepsilon_0$  any point  $x$  of the thin part with  $|x| < \varepsilon$  is on an essential loop in  $X \setminus \{0\}$  of length  $\leq |x|^q$ .*

In fact one can prove more (but we will not do so here): the set of points which are on essential loops as in the above theorem gives the thin part of a minimal thick-thin decomposition when intersected with a sufficiently small  $B_\varepsilon$ .

We have already pointed out that the thick-thin decomposition is an invariant of a semi-algebraic bilipschitz homeomorphism. But in fact, if one makes an arbitrary  $K$ -bilipschitz change to the metric on  $X$ , the thin pieces can still be recovered up to homeomorphism using the construction of the previous paragraph plus some 3-manifold

topology to tidy up the result. Again, we omit details.

### 9. Metric tangent cone

The thick-thin decomposition gives a description of the metric tangent cone of Bernig and Lytchak [1] for a normal complex surface germ. The *metric tangent cone*  $\mathcal{T}_0A$  is defined for any real semi-algebraic germ  $(A, 0) \subset (\mathbb{R}^N, 0)$  as the Gromov–Hausdorff limit

$$\mathcal{T}_0A := \lim_{\varepsilon \rightarrow 0}^{\text{GH}} \left( \frac{1}{\varepsilon}A, 0 \right),$$

where  $(1/\varepsilon)A$  means  $A$  with its inner metric scaled by a factor of  $1/\varepsilon$ .

As a metric germ,  $\mathcal{T}_0A$  is the strict cone on its link  $\mathcal{T}_0A^{(1)} := \mathcal{T}_0A \cap S_1$ , and

$$\mathcal{T}_0A^{(1)} = \lim_{\varepsilon \rightarrow 0}^{\text{GH}} \frac{1}{\varepsilon}A^{(\varepsilon)},$$

where  $(1/\varepsilon)A^{(\varepsilon)}$  is the link of radius  $\varepsilon$  of  $(A, 0)$  scaled to lie in the unit sphere  $S_1 \subset \mathbb{R}^N$ .

Applying this to  $(X, 0) \subset \mathbb{C}^n$ , we see that the thin zones collapse to circles as  $\varepsilon \rightarrow 0$ . In particular, the boundary tori of each Seifert manifold link  $(1/\varepsilon)Y_i^{(\varepsilon)}$  of a thick zone collapse to the same circles, so that in the limit we have a “branched Seifert manifold” (where branching of  $k > 1$  sheets of the manifold meeting along a circle occurs if the collapsing map of a boundary torus to  $S^1$  has fibers consisting of  $k > 1$  circles). Therefore, the link  $\mathcal{T}_0X^{(1)}$  of the metric tangent cone is the union of the branched Seifert manifolds glued along the circles to which the thin zones have collapsed.

The ordinary tangent cone  $T_0X$  and its link  $T_0X^{(1)}$  can be similarly constructed as the Hausdorff limit of  $(1/\varepsilon)X$ , resp.  $(1/\varepsilon)X^{(\varepsilon)}$  (as embedded metric spaces in  $\mathbb{C}^n$ , resp. the unit sphere  $S_1$ ). In particular, there is a canonical finite-to-one projection  $\mathcal{T}_0X \rightarrow T_0X$  (described in the more general semi-algebraic setting in [1]), whose degree over a general point  $p \in T_0X$  is the multiplicity of  $T_0X$  at that point. This is a branched cover, branched over the exceptional tangent lines in  $T_0X$ .

The circles to which thin zones collapse map to the links of some of these exceptional tangent lines, but there can also be branching in the part of  $\mathcal{T}_0X$  corresponding to the thick part of  $X$ ; such branching corresponds to bamboos on  $\mathcal{L}$ -nodes of the resolution of  $X$  of §2 or to basepoints of the family of polars which are smooth points of  $\pi^{-1}(0)$  on  $\mathcal{L}$ -curves. Summarizing, we have the following result.

**THEOREM 9.1.** *The metric tangent cone  $\mathcal{T}_0X$  is a cover of the tangent cone  $T_0X$  branched over some of the exceptional lines in  $T_0X$ . It has a natural complex structure (lifted from  $T_0X$ ) as a non-normal complex surface. Removing a finite set of complex*



lines (corresponding to thin zones) results in a complex surface which is homeomorphic to the interior of the thick part of  $X$  by a homeomorphism which is bilipschitz outside an arbitrarily small cone neighborhood of the removed lines.

**Part II: The bilipschitz classification**

The remainder of the paper builds on the thick-thin decomposition to complete the bilipschitz classification, as described in Theorem 1.9.

**10. The refined decomposition of  $(X, 0)$**

The decomposition of  $(X, 0)$  for the classification theorem (Theorem 1.9) was described there in terms of the link  $X^{(\varepsilon)}$  as follows: first refine the thick-thin decomposition

$$X^{(\varepsilon)} = \bigcup_{i=1}^r Y_i^{(\varepsilon)} \cup \bigcup_{j=1}^s Z_j^{(\varepsilon)}$$

by decomposing each thin zone  $Z_j^{(\varepsilon)}$  into its JSJ decomposition (minimal decomposition into Seifert fibered manifolds glued along their boundaries), while leaving the thick zones  $Y_i^{(\varepsilon)}$  as they are; then thicken some of the gluing tori of this refined decomposition to collars  $T^2 \times I$ . We will call the latter *special annular* pieces.

In this section we describe where these special annular pieces are added, to complete the description of the data (1) of Theorem 1.9.

We consider a generic linear projection  $\ell: (X, 0) \rightarrow (\mathbb{C}^2, 0)$  and we denote again by  $\Pi$  its polar curve and by  $\Pi^*$  the strict transform with respect to the resolution defined in §2. Before adding the special annular pieces, each piece of the above refined decomposition is either a thick zone, corresponding to an  $\mathcal{L}$ -node of our resolution graph  $\Gamma$ , or a Seifert fibered component of the minimal decomposition of a thin zone, which corresponds to a  $\mathcal{T}$ -node of  $\Gamma$ . The incidence graph for this decomposition is the graph whose vertices are the nodes of  $\Gamma$  and whose edges are the maximal strings  $\sigma$  between nodes. We add a special annular piece corresponding to a string  $\sigma$  if and only if  $\Pi^*$  meets an exceptional curve belonging to this string.

This refines the incidence graph of the decomposition by adding a vertex on each edge which gives a special annular piece. As in the introduction, we call this graph  $\Gamma_0$ . We then have a decomposition

$$X^{(\varepsilon)} = \bigcup_{\nu \in V(\Gamma_0)} M_\nu^{(\varepsilon)}, \tag{10.1}$$

into Seifert fibered components, some of which are special annular.

In the next section we will use this decomposition, together with the additional data described in Theorem 1.9, to construct a bilipschitz model for  $(X, 0)$ . To do so we will need to modify the decomposition (10.1) by replacing each separating torus of the decomposition by a toral annulus  $T^2 \times I$ :

$$X^{(\varepsilon_0)} = \bigcup_{\nu \in V(\Gamma_0)} M_\nu^{(\varepsilon_0)} \cup \bigcup_{\sigma \in E(\Gamma_0)} A_\sigma^{(\varepsilon_0)}. \quad (10.2)$$

At this point the only data of Theorem 1.9 which have not been described are the weights  $q_\nu$  of part (3). These are certain Puiseux exponents of the discriminant curve  $\Delta$  of the generic plane projection of  $X$ , and will be revealed in §12 and §13, where we show that  $X$  is bilipschitz homeomorphic to its bilipschitz model. Finally, we prove that the data are bilipschitz invariants of  $(X, 0)$  in §14.

### 11. The bilipschitz model of $(X, 0)$

We describe how to build a bilipschitz model for a normal surface germ  $(X, 0)$  by gluing individual pieces using the data of Theorem 1.9. Each piece will be topologically the cone on some manifold  $N$  and we call the subset which is the cone on  $\partial N$  the *cone-boundary* of the piece. The pieces will be glued to each other along their cone-boundaries using isometries. We first define the pieces.

*Definition 11.1.* ( $A(q, q')$ ) Here  $1 \leq q < q'$  are rational numbers.

Let  $A$  be the euclidean annulus  $\{(\varrho, \psi) : 1 \leq \varrho \leq 2 \text{ and } 0 \leq \psi \leq 2\pi\}$  in polar coordinates and for  $0 < r \leq 1$  let  $g_{q, q'}^{(r)}$  be the following metric on  $A$ :

$$g_{q, q'}^{(r)} := (r^q - r^{q'})^2 d\varrho^2 + ((\varrho - 1)r^q + (2 - \varrho)r^{q'})^2 d\psi^2.$$

So  $A$  with this metric is isometric to the euclidean annulus with inner and outer radii  $r^{q'}$  and  $r^q$ . The metric completion of  $(0, 1] \times S^1 \times A$  with the metric

$$dr^2 + r^2 d\theta^2 + g_{q, q'}^{(r)}$$

compactifies it by adding a single point at  $r=0$ . We call the result  $A(q, q')$ .

(To make the comparison with the local metric of Nagase [32] clearer, we note that this metric is bilipschitz equivalent to

$$dr^2 + r^2 d\theta^2 + r^{2q}(ds^2 + (r^{q'-q} + s)^2 d\psi^2)$$

with  $s = \varrho - 1$ .)

*Definition 11.2.* ( $B(F, \phi, q)$ ) Let  $F$  be a compact oriented 2-manifold,  $\phi: F \rightarrow F$  be an orientation-preserving diffeomorphism, and  $F_\phi$  be the mapping torus of  $\phi$  defined as

$$F_\phi := ([0, 2\pi] \times F) / ((2\pi, x) \sim (0, \phi(x))).$$

Given a rational number  $q > 1$ , we will define a metric space  $B(F, \phi, q)$ , which is topologically the cone on the mapping torus  $F_\phi$ .

For each  $0 \leq \theta \leq 2\pi$  choose a Riemannian metric  $g_\theta$  on  $F$ , varying smoothly with  $\theta$ , such that, for some small  $\delta > 0$ ,

$$g_\theta = \begin{cases} g_0 & \text{for } \theta \in [0, \delta], \\ \phi^* g_0 & \text{for } \theta \in [2\pi - \delta, 2\pi]. \end{cases}$$

Then, for any  $r \in (0, 1]$ , the metric  $r^2 d\theta^2 + r^{2q} g_\theta$  on  $[0, 2\pi] \times F$  induces a smooth metric on  $F_\phi$ . Thus

$$dr^2 + r^2 d\theta^2 + r^{2q} g_\theta$$

defines a smooth metric on  $(0, 1] \times F_\phi$ . The metric completion of  $(0, 1] \times F_\phi$  adds a single point at  $r=0$ . Denote this completion by  $B(F, \phi, q)$ . (It can be thought of as a “globalization” of the local metric of Hsiang and Pati [16]).

Note that changing  $\phi$  by an isotopy or changing the initial choice of the family of metrics on  $F$  does not change the bilipschitz class of  $B(F, \phi, q)$ . It will be convenient to make some additional choices. For a boundary component  $\partial_i F$  of  $F$  let  $m_i(F)$  be the smallest  $m > 0$  for which  $\phi^m(\partial_i F) = \partial_i F$ . By changing  $\phi$  by an isotopy if necessary and choosing the  $g_\theta$  suitably, we may assume that

- $\phi^{m_i(F)}$  is the identity on  $\partial_i F$  for each  $i$ ;
- in a neighborhood of  $\partial F$  we have  $g_\theta = g_0$  for all  $\theta$ ;
- the lengths of the boundary components of  $F$  are  $2\pi$ .

Then the metric  $r^2 d\theta^2 + r^{2q} g_\theta$  on the boundary component of  $F_\phi$  corresponding to  $\partial_i F$  is the product of a circle of circumference  $2\pi m_i(F)r$  and one of circumference  $2\pi r^q$ .

*Definition 11.3.* (CM) Given a compact smooth 3-manifold  $M$ , choose a Riemannian metric  $g$  on  $M$  and consider the metric  $dr^2 + r^2 g$  on  $(0, 1] \times M$ . The completion of this adds a point at  $r=0$ , giving a *metric cone* on  $M$ . The bilipschitz class of this metric is independent of the choice of  $g$ , and we will choose it later to give the boundary components of  $M$  specific desired shapes.

A piece bilipschitz equivalent to  $A(q, q')$  will also be said to be “of type  $A(q, q')$ ”, or briefly “of type  $A$ ”, and similarly for types  $B(F, \phi, q)$  and CM. We now describe how to glue together pieces of these three types to obtain our bilipschitz model for  $(X, 0)$ .

Note that, although we are only interested in metrics up to bilipschitz equivalence, we must glue pieces by strict isometries of their cone-boundaries. In order that the cone-boundaries are strictly isometric, we may need to change the metric in Definitions 11.2 and 11.3 by replacing the term  $r^2 d\theta^2$  by  $m^2 r^2 d\theta^2$  for some positive integer  $m$ . This gives the same metric up to bilipschitz equivalence.

For example, given  $F$ ,  $\phi$ ,  $q$  and  $q'$ , each component  $C$  of the cone-boundary of  $B(F, \phi, q)$  is isometric to the left boundary component of  $A(q, q')$  after altering the metrics on  $B(F, \phi, q)$  and  $A(q, q')$  as just described, using  $m$  equal to the number of components of  $F$  and the number of components of  $F \cap C$ , respectively. So we can glue  $B(F, \phi, q)$  to  $A(q, q')$  along  $C$ , giving a manifold with piecewise smooth metric. Similarly, a piece  $B(F, \phi, q')$  can be glued to the right boundary of  $A(q, q')$ . Finally, since the left boundary of a piece  $A(1, q')$  is strictly conical, it can be glued to a boundary component of a conical piece CM (again, after suitably adjusting the metric to be correct on the appropriate boundary component of  $M$ ).

Consider now the decomposition (10.2) of the previous section, which is the decomposition of part (1) of Theorem 1.9 but with the gluing tori thickened to annular pieces. We consider also the weights  $q_\nu$  of part (3) of Theorem 1.9.

Recall that, except for adding annular pieces, this decomposition is obtained from the thick-thin decomposition by JSJ-decomposing the thin zones.

*Remark 11.4.* Any JSJ decomposition can be positioned uniquely up to isotopy to be transverse to the foliation by fibers of a fibration over  $S^1$  (as long as the leaves are not tori). Indeed, by the transversality lemma of Roussarie [40] and Thurston [46], we can modify the JSJ decomposition by an isotopy in such a way that each separating torus and boundary torus is transversal to all leaves of the foliation. Then, using Waldhausen [48, Satz 2.8], we may assume that, up to bilipschitz equivalence, the leaves are transversal to the Seifert fibers in each Seifert fibered component.

In particular, this applies to the foliation of part (2) of Theorem 1.9, so we have a foliation with compact leaves on each non-thick piece of this decomposition. For a piece  $A_\sigma^{(\varepsilon_0)}$  the leaves are annuli and we define

$$\hat{A}_\sigma := A(q_\nu, q_{\nu'}),$$

where  $\nu$  and  $\nu'$  are nodes at the ends of the string  $\sigma$ , ordered so that  $q_\nu < q_{\nu'}$ . For a non-thick piece  $M_\nu^{(\varepsilon)}$  the leaves are fibers of a fibration  $M_\nu^{(\varepsilon)} \rightarrow S^1$ . In this case let  $\phi_\nu: F_\nu \rightarrow F_\nu$  be the monodromy map of this fibration and define

$$\hat{M}_\nu := B(F_\nu, \phi_\nu, q_\nu).$$

Finally, for each node  $\nu$  of  $\Gamma$  such that  $q_\nu=1$  (i.e.,  $M_\nu^{(\varepsilon)}$  is thick) we define

$$\widehat{M}_\nu := CM_\nu^{(\varepsilon)}.$$

We can glue together the pieces  $\widehat{M}_\nu$  and  $\widehat{A}_\sigma$  according to the topology of the decomposition  $X^{(\varepsilon)} = \bigcup_\nu M_\nu^{(\varepsilon)} \cup \bigcup_\sigma A_\sigma^{(\varepsilon)}$ , arranging, as described above, that the gluing is by isometries of the cone-boundaries. We can also make sure that the foliations match to give the foliations of the thin zones (item (2) of Theorem 1.9). We obtain a semi-algebraic set

$$(\widehat{X}, 0) = \bigcup_\nu (\widehat{M}_\nu, 0) \cup \bigcup_\sigma (\widehat{A}_\sigma, 0).$$

The next two sections prove that  $(\widehat{X}, 0)$  is bilipschitz equivalent to  $(X, 0)$  while determining the  $q_\nu$ 's of item (3) of Theorem 1.9 in the process. The proof of the theorem will then be completed in §14 by showing that the data of Theorem 1.9 are bilipschitz invariants of  $(X, 0)$ .

### 12. Carrousel decomposition and lifting

In this section, we will define a decomposition of  $(X, 0)$  into  $A$ -,  $B$ - and  $CM$ -pieces such that the polar wedges  $A_0$  (see Proposition 3.4) are  $B(D^2, \text{id}, s)$  pieces. In order to do this, we define such a decomposition of  $\mathbb{C}^2$  with respect to the discriminant curve  $\Delta$  of a generic projection  $\ell: (X, 0) \rightarrow (\mathbb{C}^2, 0)$  and we then lift this decomposition by  $\ell$ .

We assume as usual that  $\ell = (z_1, z_2)$  is a generic linear projection. We will again work inside the Milnor balls with corners  $B_\varepsilon$  defined in §4. We denote by  $(x, y)$  the coordinates in  $\mathbb{C}^2$  (so  $(x, y) = (z_1, z_2)$ ).

We first define the decomposition inside a conical neighborhood of each tangent line to  $\Delta$ . Let  $L_1, \dots, L_m$  be the tangent lines to the discriminant curve  $\Delta$  of  $\ell$ . For each  $j=1, \dots, m$ , let  $\Delta_j$  be the union of branches of  $\Delta$  which are tangent to  $L_j$  and assume that  $L_j$  is the line  $y = \lambda_j x$ . We consider a cone  $V_j = \{(x, y) : |x| \leq \varepsilon \text{ and } |y - \lambda_j x| \leq \eta |x|\} \subset \mathbb{C}^2$  centered at  $L_j$  such that  $\Delta_j \cap B_\varepsilon$  lies inside  $V_j$ .

Following the ideas of Lê [19] (see also [21]), we first construct a “carrousel decomposition” of each  $V_j$ ,  $j=1, \dots, m$ , with respect to the branches of  $\Delta_j$ . It will consist of closures of regions between successively smaller neighborhoods of the successive Puiseux approximations of the branches of  $\Delta_j$ . As such, it is finer than the one of [19], which only needed the first Puiseux pairs of the branches of  $\Delta_j$ .

For simplicity, we assume first that  $\Delta_j$  has just one branch. The curve  $\Delta_j$  admits a Puiseux series expansion of the form

$$y = \sum_{i \geq 1} a_i x^{p_i} \in \mathbb{C}\{x^{1/N}\}.$$

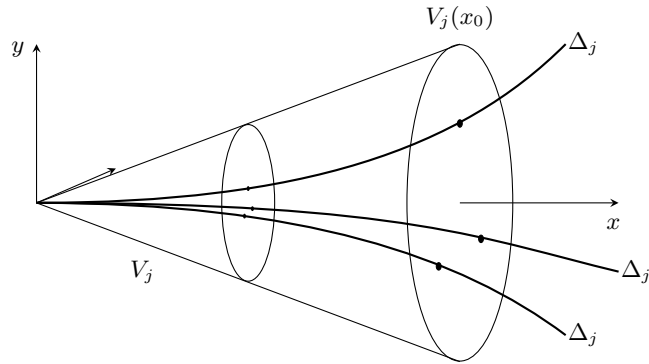


Figure 4. The cone  $V_j$  and the curve  $\Delta_j$ .

Let  $p_n = s$  be the contact exponent (see Proposition 3.4).

For each  $k \leq n$  choose  $\alpha_k, \beta_k, \gamma_k > 0$  with  $\alpha_k < |a_k| - \gamma_k < |a_k| + \gamma_k < \beta_k$  and consider the region

$$B_k := \left\{ (x, y) : \alpha_k |x^{p_k}| \leq \left| y - \sum_{i=1}^{k-1} a_i x^{p_i} \right| \leq \beta_k |x^{p_k}| \text{ and } \left| y - \sum_{i=1}^k a_i x^{p_i} \right| \geq \gamma_k |x^{p_k}| \right\}.$$

If the  $\varepsilon$  of our Milnor ball  $B_\varepsilon$  is small enough, the  $B_j$ 's will be pairwise disjoint. Denote by  $A_1$  the closure of the region between  $\partial V_j$  and  $B_1$ , and by  $A_i$  the closure of the region between  $B_{i-1}$  and  $B_i$  for  $i = 1, \dots, n$ . Finally let  $D$  be

$$D := \overline{V_j} \setminus \left( \bigcup_{i=1}^n A_i \cup \bigcup_{i=1}^n B_i \right),$$

which is the union of the connected pieces  $D_1, \dots, D_n, D_{n+1}$ , disjoint except at 0, and indexed so that  $D_k$  is adjacent to  $B_k$  and  $D_{n+1} \setminus \{0\}$  intersects  $\Delta$ .

Then, for  $k = 1, \dots, n$ ,  $A_k$  is bilipschitz equivalent to  $A(p_{k-1}, p_k)$  (Definition 11.1; we put  $p_0 = 1$ ), and  $B_k$  is bilipschitz equivalent to  $B(F_k, \phi_k, p_k)$  (Definition 11.2), where  $F_k$  is a planar surface with

$$2 + \frac{\text{lcm}_{i \leq k} \text{denom}(p_i)}{\text{lcm}_{i < k} \text{denom}(p_i)}$$

boundary components and  $\phi_k$  is a finite-order diffeomorphism. Finally, each  $D_k$  is bilipschitz to  $B(D^2, \text{id}, p_k)$ .

More generally, if  $\Delta_j$  has several components, we first truncate the Puiseux series for each component of  $\Delta_j$  at its contact exponent. Then for each pair  $\varkappa = (f, p_k)$  consisting of a Puiseux polynomial  $f = \sum_{i=1}^{k-1} a_i x^{p_i}$  and an exponent  $p_k$  for which  $f = \sum_{i=1}^k a_i x^{p_i}$  is a partial sum of the truncated Puiseux series of some component of  $\Delta_j$ , we consider

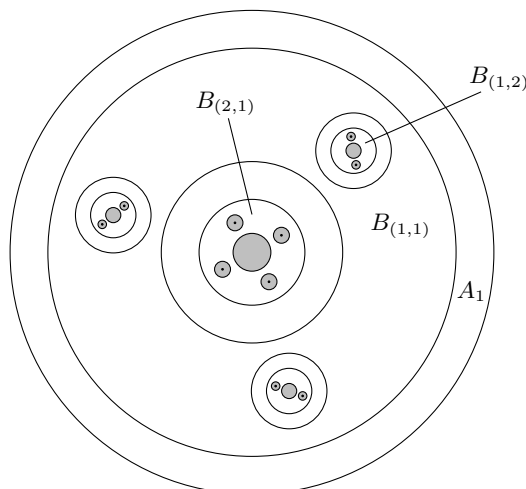


Figure 5. Carrousel section for  $\Delta = \{(x, y) : y = ax^{4/3} + bx^{13/6} + \dots\} \cup \{(x, y) : y = cx^{7/4} + \dots\}$ . The region  $D$  is gray.

all components of  $\Delta_j$  which fit this data. If  $a_{k1}, \dots, a_{kt}$  are the coefficients of  $x^{pk}$  which occur in these Puiseux polynomials we define

$$B_{\varkappa} := \left\{ (x, y) : \alpha_{\varkappa} |x^{pk}| \leq \left| y - \sum_{i=1}^{k-1} a_i x^{p_i} \right| \leq \beta_{\varkappa} |x^{pk}| \right.$$

$$\left. \text{and } \left| y - \left( \sum_{i=1}^{k-1} a_i x^{p_i} + a_{kj} x^{p_k} \right) \right| \geq \gamma_{\varkappa} |x^{pk}| \text{ for } j = 1, \dots, t \right\}.$$

Here  $\alpha_{\varkappa}$ ,  $\beta_{\varkappa}$  and  $\gamma_{\varkappa}$  are chosen so that  $\alpha_{\varkappa} < |a_{kj}| - \gamma_{\varkappa} < |a_{kj}| + \gamma_{\varkappa} < \beta_{\varkappa}$  for each  $j = 1, \dots, t$ . Again, if the  $\varepsilon$  of our Milnor ball is small enough, the sets  $B_{\varkappa}$  will be disjoint for different  $\varkappa$ , and each is again bilipschitz equivalent to some  $B(F, \phi, p_k)$  with  $\phi$  of finite order. The closure of the complement in  $V_j$  of the union of the  $B_{\varkappa}$ 's is again a union of pieces bilipschitz equivalent to some  $A(q, q')$  or some  $B(D^2, \text{id}, q)$ .

The carrousel picture is the picture of the intersection of this decomposition of the cone  $V_j$  with the plane  $x = \varepsilon$ . Figure 5 shows this picture for a discriminant  $\Delta_j$  having two branches with Puiseux series expansions up to their contact exponents  $y = ax^{4/3} + bx^{13/6}$  and  $y = cx^{7/4}$ , respectively. Note that the intersection of a piece of the decomposition of  $V_j$  with the disk  $V_j \cap \{(x, y) : x = \varepsilon\}$  will usually have several components.

We now take a decomposition as above in each of the cones  $V_j$  and add the additional piece  $Y := \left( \mathbb{C}^2 \setminus \bigcup_{j=1}^t V_j, 0 \right)$  to get a decomposition of all of  $(\mathbb{C}^2, 0)$ . This piece  $Y$  is conical, i.e., of type CM.

We next describe a lifting by  $\ell$  of this decomposition of  $(\mathbb{C}^2, 0)$  to  $(X, 0)$ .

For each  $j$  denote by  $\Delta_{j1}, \dots, \Delta_{jk_j}$  the components of the discriminant which are in  $V_j$  and  $B'_{j1}, \dots, B'_{jk_j}$  the corresponding sets described in the remark following Proposition 3.4. Let  $A_{j1}, \dots, A_{jk_j}$  be the corresponding polar wedges, described as components of the inverse images of the  $B'_{ji}$  (as in Proposition 3.4 (2) and the remark following it), with contact exponents  $s_{j1}, \dots, s_{jk_j}$ .

Notice that each  $B'_{ji}$  is a union of carousel pieces. In particular, if  $k_j=1$ , so that the part of the discriminant in  $V_j$  is irreducible, then it is a piece of type  $B(D^2, \text{id}, s_{j0})$ .

Set

$$(X^L, 0) := \left( X \setminus \bigcup_{j=1}^t \bigcup_{i=1}^{k_j} A_{ji}, 0 \right),$$

and let  $\ell^L: (X^L, 0) \rightarrow (\mathbb{C}^2, 0)$  be the restriction of  $\ell: (X, 0) \rightarrow (\mathbb{C}^2, 0)$ .

LEMMA 12.1. (1) *Each polar wedge  $A_{ji}$  is a piece of type  $B(D^2, \text{id}, s_{ji})$ .*

(2) *The inverse image by  $\ell^L$  of the CM piece  $Y$  of the carousel is a union of CM pieces. The inverse image by  $\ell^L$  of any  $A(q, q')$  piece of the carousel is a disjoint union of  $A(q, q')$  pieces. The inverse image by  $\ell^L$  of any  $B(F, \phi, q)$  piece is a disjoint union of pieces of type  $B(F, \phi, q)$  (with the same  $q$  but usually different  $F$ 's and  $\phi$ 's), and the  $\phi$ 's for these pieces have finite order, so their links are Seifert fibered.*

*Proof.* Part (1) is proved in Proposition 3.4. In part (2) each inverse image piece is an unbranched cover of a piece of the carousel, with metric bilipschitz equivalent to the lifted metric, so this part of the lemma follows.  $\square$

We have now constructed a decomposition of  $(X, 0)$  into “model pieces” but the decomposition is not minimal. We will next describe how to simplify it step by step, leading to a decomposition equivalent to the the one described in §11.

### 13. Bilipschitz equivalence with the model

We will start with the above non-minimal decomposition of  $(X, 0)$  into model pieces and then simplify it until it is minimal. This will use the following trivial lemma, which gives rules for simplifying a decomposition into model pieces. The reader can easily add more rules; we intentionally list only the ones we use.

LEMMA 13.1. *In this lemma  $\cong$  means bilipschitz equivalence and  $\cup$  represents gluing along appropriate boundary components by an isometry.*

(1)  $B(D^2, \phi, q) \cong B(D^2, \text{id}, q)$  and  $B(S^1 \times I, \phi, q) \cong B(S^1 \times I, \text{id}, q)$ .

(2)  $A(q, q') \cup A(q', q'') \cong A(q, q'')$ .



(3) If  $F$  is the result of gluing a surface  $F'$  to a disk  $D^2$  along boundary components, then  $B(F', \phi|_{F'}, q) \cup B(D^2, \phi|_{D^2}, q) \cong B(F, \phi, q)$ .

(4)  $A(q, q') \cup B(D^2, \text{id}, q') \cong B(D^2, \text{id}, q)$ .

(5) Each  $B(D^2, \text{id}, 1)$ ,  $B(S^1 \times I, \text{id}, 1)$  or  $B(F, \phi, 1)$  piece is a CM piece, and a union of CM pieces glued along boundary components is a CM piece.

We will apply these rules repeatedly to amalgamate pieces in  $(X, 0)$ . But first we will introduce a restriction on the use of rule (2) which will avoid the amalgamation of some specific annular pieces.

Notice that in rule (2) (as well as in rule (4)), there is no restriction on  $q$ ,  $q'$  and  $q''$ . In particular,  $q=q'$  or  $q'=q''$ , i.e., amalgamation of  $A(q', q')$  pieces, is a priori allowed. In the carousel decomposition of  $(\mathbb{C}^2, 0)$  annular pieces of type  $A(q, q')$  only occur with  $q < q'$ , but in  $(X, 0)$  a  $B(S^1 \times I, \text{id}, q')$  piece (which can be thought of as a piece of type  $A(q', q')$ ) can arise when amalgamating lifted pieces. The following lemma clarifies how such  $A(q', q')$  pieces can arise in the decomposition of  $(X, 0)$ .

LEMMA 13.2. *If an annular piece of type  $A(q', q')$  arises in  $(X, 0)$  it is either*

(1) *an unbranched cover of an annular region of the carousel (arising as a union of a  $B$ -piece along with the pieces which “fill the holes” of this  $B$ -piece), or*

(2) *a branched cover of a region of type  $B(D^2, \text{id}, q)$  in the carousel.*

*In case (1) the two adjacent pieces to the  $A(q', q')$  piece are of type  $A(q, q')$  and  $A(q', q'')$  with  $q < q' < q''$ , while in case (2) the two adjacent pieces are of type  $A(q, q')$  with  $q < q'$ .*

*Proof.* For the piece to be annular its intersection with a Milnor fiber (i.e., intersection with  $\{(z_1, \dots, z_n): z_1 = x_0\}$ ) must be a union of annuli  $S^1 \times I$ . Euler characteristic shows that an annulus can branch cover only an annulus (with no branching) or a disk. The two possibilities give the two cases in the lemma. The statement about adjacent pieces is seen by considering the adjacent pieces to the image of the  $A(q', q')$  piece in  $(\mathbb{C}^2, 0)$ . □

A piece as in item (2) of Lemma 13.2 is a *special annular piece*. We will now apply the rules of Lemma 13.1 to amalgamate pieces of the decomposition, with the following additional rule:

(6) A special annular piece is never amalgamated with another piece.

The amalgamation process stops when there is no  $B(D^2, \text{id}, q)$  piece left, no piece of type  $A(q, q)$  which is not special annular, no pairs of adjacent annular pieces which are not special annular, and no pairs of adjacent CM pieces. At each step of the process there is at least one piece of type  $A(q, q')$  between any two pieces of type CM,  $B(F, \phi, q)$

with  $F \neq D^2$ , or special annular. So at the end of the process we just have pieces of these three types with  $A(q, q')$  pieces separating them.

We call this decomposition the *classifying decomposition of  $(X, 0)$*  and we create an incident graph  $\Gamma_0$  for it with a vertex for each connected piece which is of type CM,  $B$  or special annular, and with an edge for each annular piece connecting two such pieces.

LEMMA 13.3.  $\Gamma_0$  is the graph  $\Gamma_0$  of Theorem 1.9 and §10.

*Proof.* Note first that rule (5) of Lemma 13.1 absorbs into the initial CM pieces (components  $\ell^{-1}(Y)$ , where  $Y := (\mathbb{C}^2 \setminus \bigcup_j V_j, 0)$ ) any adjacent  $D$ -type piece. These are any component of an  $\ell^{-1}(V_i)$  which maps by a covering map to  $V_i$ , any piece coming from a moving polar (see the proof of part (1) of Lemma 6.2) and any piece coming from a bamboo on an  $\mathcal{L}$ -node. In particular, part (3) of Lemma 6.2 is proved, and we also see that the CM pieces of the classifying decomposition are exactly the “conical cores” of the thick pieces of the thick-thin decomposition (i.e., when amalgamated with the adjacent annular pieces of type  $A(1, q)$ , they are the thick pieces).

After removing the thick pieces we are left with the thin pieces, and for each thin piece  $Z_j$  and its link  $Z_j^{(\varepsilon)}$  we need to show the following:

- (i) if one ignores the annular and special annular pieces, the decomposition of  $Z_j^{(\varepsilon)}$  is its minimal decomposition into Seifert fibered components;
- (ii) there is a special annular piece between two Seifert fibered components if and only if the strict transform of the polar meets the corresponding string of rational curves in the resolution graph.

For (i), note that the JSJ decomposition of a thin zone is characterized by the fact that the pieces are not annular and the Seifert fibrations of adjacent pieces do not match up to isotopy on the common torus.

For pieces which do not have a special annular piece between them this is clear: The Seifert fibrations run parallel to the curves of Puiseux approximations to the branches of the  $\Delta_j$  and are determined therefore by the weights  $q$ ; two adjacent pieces with no special annular piece between them are separated by an  $A(q, q')$  and, since  $q \neq q'$ , the fibrations do not match.

For pieces with a special annular piece between them it is also not hard to see. In this case there is an annular region between them which is composed of pieces  $A(q_1, q')$  and  $A(q_2, q')$  glued to a  $B(S^1 \times I, \text{id}, q')$  between them. We claim the mismatch of Seifert fibrations given by  $A(q_1, q')$  and  $A(q_2, q')$  accumulate rather than cancel. A geometric approach is to consider an arc in the Milnor fiber  $W_j \cap \{(z_1, \dots, z_n) : z_1 = \varepsilon e^{i\theta}\}$  from an intersection of a Seifert fiber of one piece to an intersection of the Seifert fiber of the other, and watch what happens to this arc as one swings the Milnor fiber through increasing

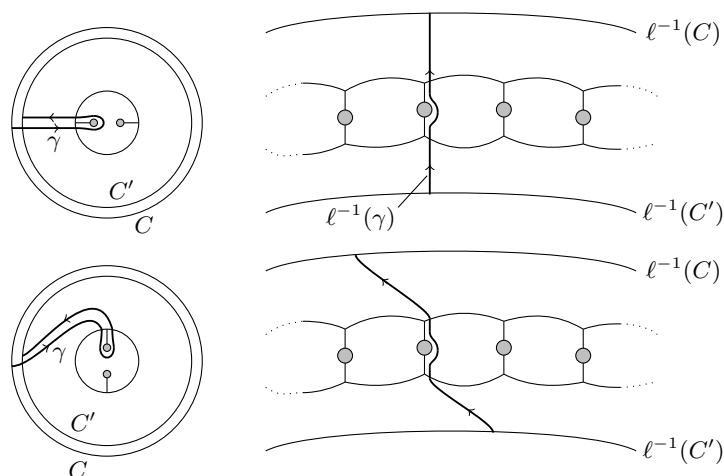


Figure 6. Non-matching of Seifert fibers across a special annular piece.

$\theta$ , keeping the arc on the Milnor fiber and its ends on their respective Seifert fibers. If the Seifert fibrations were parallel the arc would have constant length. It passes through the special annulus, and we may assume it does this efficiently, so that its image in the image disk  $V_j \cap \{(z_1, z_2) : z_1 = x_0\}$  enters near a branch point, circles the branch point, and exits. The branch points in this disk are rotating faster than the endpoints of the arc, since  $q' > q_1$  and  $q' > q_2$ , so the curve must stretch (see Figure 6).

We have proved the correspondence between the non-annular pieces of our decomposition and JSJ-components, and hence with  $\mathcal{T}$ -nodes in  $\Gamma$ . The correspondence (ii) can now be seen as follows. A string between nodes in  $\Gamma$  for which the polar meets an exceptional curve corresponds to an annulus of the Nielsen decomposition of the Milnor fiber (see Remark 7.6) which meets the polar. This means that the annulus covers its image in  $V_j \cap \{(z_1, z_2) : z_1 = x_0\}$  with non-trivial branching. By Lemma 13.2 this means that the image is a disk, so the annulus is the Milnor fiber of a special annulus.

This completes the proof that the decomposition graph for the classifying decomposition is indeed the graph  $\Gamma_0$  of Theorem 1.9 and §10.  $\square$

The vertex-weights  $q_\nu$  are the  $q$ 's of the model pieces of this constructed decomposition. They are the last data we needed to assemble to complete the data of Theorem 1.9.

This decomposition of  $X \cap B_{\varepsilon_0}$  into model pieces matches the construction of the model  $\widehat{X}$  in §11, so we have shown the following result.

**COROLLARY 13.4.** *The bilipschitz model  $\widehat{X}$  constructed in §11 using the data we have assembled for Theorem 1.9 is bilipschitz homeomorphic to  $X \cap B_{\varepsilon_0}$ .*

This corollary completes the proof of half of Theorem 1.9. It remains to show that the data of that theorem are bilipschitz invariants.

*Remark 13.5.* Each vertex  $\nu$  of  $\Gamma_0$  corresponds either to a node of  $\Gamma$  or, in the case of a special annular piece, to a maximal string  $\sigma$  of  $\Gamma$  which contains a vertex corresponding to an exceptional curve which intersect  $\Pi^*$  (we call the minimal substring of  $\sigma$  containing all such vertices an  $\mathcal{A}$ -string, and also an  $\mathcal{A}$ -node if it is a single vertex). In discussing examples, it is often more convenient to associate the weight  $q_\nu$  with the corresponding node or  $\mathcal{A}$ -string of  $\Gamma$ .

Any rate  $q_\nu$  is either 1 or is a characteristic exponent of a branch of the discriminant curve  $\Delta$ . But in general, not all characteristic exponents appear as rates.

For example, the singularity  $(X, 0) \subset (\mathbb{C}^3, 0)$  with equation  $x^3 + y^4 + z^4$  is metrically conical (see Example 7.12), so the only rate  $q_\nu$  is 1 at the single  $\mathcal{L}$ -node. But the discriminant curve of a generic linear projection consists of four transversal cusps each with Puiseux exponent  $\frac{3}{2}$ . This also happens when the contact exponent of a branch of  $\Delta$  is strictly less than its last characteristic exponent.

There are also examples where all characteristic exponents of  $\Delta$  appear as rates  $q_\nu$  of  $\mathcal{T}$ -nodes or  $\mathcal{A}$ -strings. This is the case for any  $(X, 0)$  with equation  $z^2 - f(x, y) = 0$ , where  $f$  is irreducible. Indeed, let  $\{(r_k, q_k)\}_{k=1}^n$  be the set of Puiseux pairs of  $f$  (see [9, p. 49]), i.e., the characteristic Puiseux exponents of the curve  $f=0$  are the rational numbers  $p_k = q_k/r_1 \dots r_k$ . The projection  $\ell = (x, y)$  is generic and its discriminant curve is  $\{(x, y) : f(x, y) = 0\}$ . By [26, Propositions 4.1 and 4.2], for any  $k=1, \dots, n-1$ , each connected component of  $\ell^{-1}(B_k)$  gives rise to a  $\mathcal{T}$ -node of  $\Gamma$  with rate  $p_k$ . Moreover, either  $r_n \neq 2$ , and then  $\ell^{-1}(B_n)$  gives rise to a  $\mathcal{T}$ -node with rate  $p_n$ , or  $r_n = 2$ , and then  $\ell^{-1}(B_n)$  gives rise to an  $\mathcal{A}$ -node with rate  $p_n$ .

#### 14. Bilipschitz invariance of the data

In this section, we prove that the data (1)–(3) of Theorem 1.9 are determined by the bilipschitz geometry of  $(X, 0)$ .

We first consider the refined decomposition of  $(X, 0)$  presented in §10, which is part (1) of the data of the classification theorem (Theorem 1.9):

$$X^{(\varepsilon_0)} = \bigcup_{\nu \in \mathcal{N}_\Gamma} M_\nu^{(\varepsilon_0)} \cup \bigcup_{\sigma \in \mathcal{S}_\Gamma} A_\sigma^{(\varepsilon_0)}.$$

LEMMA 14.1. *The bilipschitz geometry of  $(X, 0)$  determines, up to homeomorphism, the above decomposition.*

*Proof.* The thick-thin decomposition

$$(X, 0) = \bigcup_{i=1}^r (Y_i, 0) \cup \bigcup_{j=1}^s (Z_j, 0)$$

is determined up to homeomorphism by the bilipschitz geometry of  $(X, 0)$  (§8). For each  $\mathcal{L}$ -node  $\nu$ , the associated thick piece  $Y_\nu$  is defined by  $Y_\nu = \pi(N(\Gamma_\nu))$  (§2). Therefore the link  $M_\nu^{(\varepsilon_0)}$ , which coincides with  $Y_\nu^{(\varepsilon_0)}$  up to a collar neighborhood, is determined by the bilipschitz geometry. For each Tjurina component  $\Gamma_j$  of  $\Gamma$ , the pieces  $M_\nu^{(\varepsilon_0)}$  corresponding to  $\mathcal{T}$ -nodes in  $\Gamma_j$  are exactly the Seifert components of the minimal JSJ decomposition of  $Z_j^{(\varepsilon_0)}$ . Since the minimal JSJ decomposition of a 3-manifold is unique up to isotopy, the pieces  $M_\nu$  are determined up to homeomorphism by the bilipschitz geometry.

It remains to prove that the special annular pieces  $A_\sigma^{(\varepsilon_0)}$  are also determined by the bilipschitz geometry. This will be done in Lemma 14.4 □

We next prove the bilipschitz invariance of data (2) of Theorem 1.9.

LEMMA 14.2. *The bilipschitz geometry of  $(X, 0)$  determines for each thin zone  $Z_j^{(\varepsilon)}$  the foliation of  $Z_j^{(\varepsilon)}$  by fibers of  $\zeta_j^{(\varepsilon)}$ .*

*Proof.* We begin with a remark: If  $M \rightarrow S^1$  is a fibration of a compact connected oriented 3-manifold, we consider  $M$  as a foliated manifold, with compact leaves which are the connected components of the fibers. If the fibration has disconnected fibers, then it is the composition with a covering map  $S^1 \rightarrow S^1$  of a fibration with connected fiber  $F$ . This fibration gives the same foliation (and it is determined up to isotopy by  $F \subset M$ ). We recall also that the isotopy class of a fibration  $\zeta: M \rightarrow S^1$  of a 3-manifold is determined up to isotopy by the homotopy class  $[\phi] \in [M, S^1] = H^1(M; \mathbb{Z})$  and has connected fibers if and only if this class is primitive. (See, e.g., [44].)

According to Proposition 5.1, the fibration  $\zeta_j^{(\varepsilon)}: Z_j^{(\varepsilon)} \rightarrow S_\varepsilon^1$  varies continuously with  $\varepsilon$ , and the diameter of the fibers shrinks faster than linearly with  $\varepsilon$ . As just described, we can modify  $\zeta_j^{(\varepsilon)}$  if necessary to have a connected fiber  $F_j$  without changing the foliation by fibers. Any fibration  $\xi: Z_j^{(\varepsilon)} \rightarrow S^1$  generating a different foliation up to isotopy has fibers which map essentially (i.e., not null-homotopically) to  $S^1$  by  $\zeta_j^{(\varepsilon)}$ , so their diameter cannot shrink superlinearly with  $\varepsilon$ . Hence our foliation is determined up to isotopy by the bilipschitz geometry. □

Recall that a closed curve (or “loop”) in  $X \setminus \{0\}$  is *essential* if it is not null-homotopic in  $X \setminus \{0\}$ . A continuous family of essential loops  $\{\gamma_\varepsilon: S^1 \rightarrow X^{(\varepsilon)}\}_{0 < \varepsilon \leq \varepsilon_0}$  is a *fast loop* (of the first kind) if the lengths shrink faster than linearly in  $\varepsilon$ . If  $\text{length}(\gamma_\varepsilon) = O(\varepsilon^q)$  we call  $q$  the *rate* of the fast loop.

LEMMA 14.3. *For a Tjurina component  $\Gamma_j$  of  $\Gamma$  and a  $\mathcal{T}$ -node  $\nu$  in  $\Gamma_j$ , denote by  $F_\nu^{(\varepsilon)}$  a fiber of the fibration  $\zeta_\nu^{(\varepsilon)}: M_\nu^{(\varepsilon)} \rightarrow S^1$  obtained by restricting  $\zeta_j^{(\varepsilon)}$  to  $M_\nu^{(\varepsilon)}$ . Then  $F_\nu^{(\varepsilon_0)}$  contains an essential loop which is not homotopic into  $\partial F_\nu^{(\varepsilon_0)}$ . Any such loop gives a fast loop of maximal rate  $q_\nu$ , so  $q_\nu$  is a bilipschitz invariant.*

*Proof.* Note that a fast loop can only exist in a thin zone, and then an argument similar to the proof of the lemma above shows that there is no loss of generality in considering only fast loops which are homotopic into Milnor fibers of the thin zone. Indeed, a loop which is not homotopic into a Milnor fiber must map essentially to the circle under the fibration  $\zeta_j$  and hence cannot shrink faster than linearly.

Let  $\gamma$  be a loop in  $F_\nu^{(\varepsilon_0)}$  which is neither null-homotopic in  $F_\nu^{(\varepsilon_0)}$  nor homotopic into a boundary component of  $F_\nu^{(\varepsilon_0)}$  (since  $\pi_1(F_\nu^{(\varepsilon_0)})$  is a non-abelian free group, most loops have this property). Let  $\delta$  be a boundary component of  $F_\nu^{(\varepsilon_0)}$ . We can choose  $\gamma$  so that, after connecting these loops to a base-point, neither of the loops  $\gamma$  or  $\gamma\delta$  is boundary-parallel. If both were inessential then  $\delta \sim \gamma^{-1}\gamma\delta$  would be inessential, but Proposition 7.7 says that each boundary component of  $F_\nu^{(\varepsilon_0)}$  is essential. Thus at least one of them is the desired essential loop in  $F_\nu^{(\varepsilon_0)}$ .

Since  $M_\nu$  is of type  $B(F_\nu, \phi, q_\nu)$ , it is clear that every essential loop in  $F_\nu^{(\varepsilon_0)}$  yields a fast loop of rate at least  $q_\nu$ . Now let  $\gamma$  be an essential loop in  $M_\nu^{(\varepsilon_0)}$  which is homotopic into  $F_\nu^{(\varepsilon_0)}$  but not homotopic into a boundary component of  $F_\nu^{(\varepsilon_0)}$ . Every representative of  $\gamma$  intersects  $M_\nu^{(\varepsilon_0)}$ , and there is a lower bound on the length of the portion of such a representative which lies in  $M_\nu^{(\varepsilon_0)}$ , which is realized within a fiber  $F_\nu^{(\varepsilon_0)}$ . Since  $F_\nu^{(\varepsilon_0)}$  shrinks uniformly at rate  $q_\nu$ , it follows that  $q_\nu$  is an upper bound on the rate of fast loops with  $\gamma_{\varepsilon_0} = \gamma$ . □

LEMMA 14.4. *The bilipschitz geometry of  $(X, 0)$  determines the special annular pieces  $M_\nu$  and the maximal rate  $q_\nu$  of each such piece  $M_\nu$ .*

*Proof.* Let  $\gamma$  be a boundary component of the fiber  $F_\nu$  for a  $\mathcal{T}$ -node  $\nu$  and let  $\nu'$  be the adjacent node for that boundary component. Then  $\gamma$  is a fast loop with rate at least  $\max\{q_\nu, q_{\nu'}\}$ . If there is no special annular piece between  $M_\nu$  and  $M_{\nu'}$ , the argument of the previous lemma shows that the maximal rate is exactly  $\max\{q_\nu, q_{\nu'}\}$ , while if there is a special annular piece  $M_{\nu''}$ , then it is  $q_{\nu''}$ . □

Lemmas 14.3 and 14.4 prove bilipschitz invariance of all the  $q_\nu$ 's and complete the proof of Lemma 14.1. So the proof of Theorem 1.9 is complete.

### 15. Examples

In this section, we describe the bilipschitz geometry for several examples of normal surface singularities  $(X, 0)$ . Namely, for each of them, we give the dual resolution graph  $\Gamma$  of the minimal resolution  $\pi: (\tilde{X}, E) \rightarrow (X, 0)$  considered in §10 with the additional data:

- (1') the  $\mathcal{L}$ -,  $\mathcal{T}$ - and  $\mathcal{A}$ -nodes represented by black vertices;
- (2') the arrows representing the strict transform of a generic linear form;
- (3') the rate  $q_\nu$  weighting each node  $\nu$ .

The data (1') and (3') are equivalent to (1) and (3), respectively, of Theorem 1.9.

The data (2') determines the multiplicities  $m_\nu$  of the generic linear form  $z_1$  along each exceptional curve  $E_\nu$ ,  $\nu \in \Gamma$ . In all the examples treated here, we are in one of the following two situations: either the link  $X^{(\varepsilon)}$  is a rational homology sphere, or for each node  $\nu \in \Gamma$ ,

$$\gcd\{\gcd\{m_\nu, m_\mu\} : \mu \in V_\nu\} = 1,$$

where  $V_\nu$  denotes the set of neighbor vertices of  $\nu$  in  $\Gamma$  including arrows (which have multiplicities 1). In these two situations, the multiplicities  $m_\nu$  determine the embedded topology in  $X^{(\varepsilon)}$  of the Milnor fiber of  $z_1$ , and then data (2) of Theorem 1.9 (see for example [39]).

Recall that the  $\mathcal{L}$ -nodes of  $\Gamma$  are the vertices carrying at least one arrow or, equivalently, having rate 1. The Tjurina components of  $\Gamma$  are the components obtained by removing the  $\mathcal{L}$ -nodes and adjacent edges. Then, according to §2 and Theorem 1.7, the thick-thin decomposition  $(X, 0) = (\bigcup_i (Y_i, 0)) \cup (\bigcup_j (Z_j, 0))$  of  $(X, 0)$  is read from the graph  $\Gamma$  as follows:

- The thin pieces  $(Z_j, 0)$  of  $(X, 0)$  correspond to the Tjurina components which are not bamboos.
- The thick pieces  $(Y_i, 0)$  of  $(X, 0)$  are in bijection with the  $\mathcal{L}$ -nodes of  $\Gamma$ . They correspond to the connected components of the graph obtained by removing from  $\Gamma$  the Tjurina components which are not bamboos and their adjacent edges.

Each example has been computed as follows: we start by computing the graph  $\Gamma$  with  $\mathcal{L}$ -nodes and arrows. Then, for each Tjurina component, we determine the  $\mathcal{A}$ -nodes and the rates at  $\mathcal{A}$ - and  $\mathcal{T}$ -nodes either by studying the Puiseux expansions of the branches of the discriminant curve  $\Delta$  and the cover  $\ell$ , or by determining the strict transform of the polar curve  $\Pi^*$  using the equation of  $X$  and the multiplicities of the coordinates functions in the graph, or by using Hironaka numbers (see Remark 15.3).

In Example 15.2 we will treat the case of a superisolated singularity in all detail. We start by presenting the thick-thin decomposition for this family of singularities.

*Example 15.1.* (Superisolated singularities) A hypersurface singularity  $(X, 0)$  with equation  $f_d(x, y, z) + f_{d+1}(x, y, z) + \dots = 0$ , where each  $f_k$  is a homogeneous polynomial of degree  $k$ , is *superisolated* if the projective plane curve  $C := \{(x, y, z) : f_d(x, y, z) = 0\} \subset \mathbb{P}^2$  is reduced with isolated singularities  $\{p_i\}_i$  and these points  $p_i$  are not situated on the projective curve  $\{(x, y, z) : f_{d+1}(x, y, z) = 0\}$  (see [24] and [25]). Such a singularity is resolved by the blow-up  $\pi_1$  of the origin of  $\mathbb{C}^3$ . Therefore, the thick zones are in bijection with the components of the projectivized tangent cone  $C$ . Moreover, the resolution  $\pi: (\tilde{X}, E) \rightarrow (X, 0)$  introduced in §2 is obtained by composing  $\pi_1$  with the minimal resolutions of the plane curve germs  $(C, p_i)$ , and as the curve  $C$  is reduced, no Tjurina component of  $\pi$  is a bamboo. Therefore, the thin zones are in bijection with the points  $p_i$ .

The embedded topological type of  $(X, 0)$  does not depend on the  $f_k$ ,  $k > d$ , provided  $f_{d+1} = 0$  does not contain any of the singular points  $p_i$  of  $C$ . The previous arguments show that the thick-thin decomposition of  $(X, 0)$  also only depends on  $C$  and does not change when replacing the equation by  $f_d + l^{d+1} = 0$ , where  $l$  is a generic linear form.

For example, taking  $C$  with smooth irreducible components intersecting transversely, we obtain a thick-thin decomposition whose thin zones are all thickened tori, and whose topology comes from the thick pieces (in fact the genus of the irreducible components of  $C$ ) and cycles in the resolution graph.

*Example 15.2.*  $((X, 0)$  with equation  $(zx^2 + y^3)(x^3 + zy^2) + z^7 = 0$ ) This is a superisolated singularity and we compute the resolution graph with  $\mathcal{L}$ -nodes and strict transform of the generic linear form by blowing-up the origin and then resolving the singularities of the exceptional divisor. We get two  $\mathcal{L}$ -curves intersecting at five points and one visible Tjurina component in the graph. Blowing-up the five intersection points, we then obtain five additional Tjurina components each consisting of one node between the two  $\mathcal{L}$ -nodes. We obtain the resolution graph of Figure 7. The numbers in parentheses are the multiplicities of the generic linear form while the others are the self-intersection numbers (Euler classes) of the exceptional curves.

Computing the multiplicities of a generic linear combination of  $f_x$ ,  $f_y$  and  $f_z$  as in Example 3.5, we obtain that the polar curve has 14 branches and that the resolution graph of the minimal resolution which resolves the basepoints of the family of polar curves is as in Figure 8 (the number at each vertex is the multiplicity of a generic combination  $af_x + bf_y + cf_z$ ).

Therefore, the discriminant curve  $\Delta$  of a generic linear projection  $\ell: (X, 0) \rightarrow (\mathbb{C}^2, 0)$  has 14 branches and 12 distinct tangent lines  $L_1, \dots, L_{12}$ .

Let  $\Delta_0$  be a branch of  $\Delta$  and let  $\Pi_0$  be the branch of the polar curve such that  $\ell(\Pi_0) = \Delta_0$ . The intersection of  $\Delta_0$  with the Milnor fiber of a generic form on  $\mathbb{C}^2$  is the



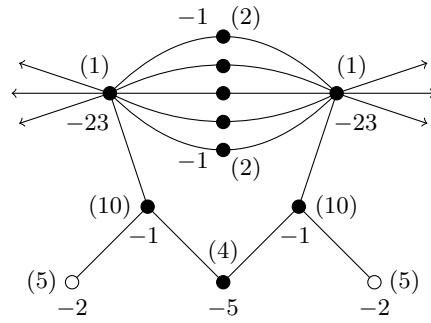


Figure 7.

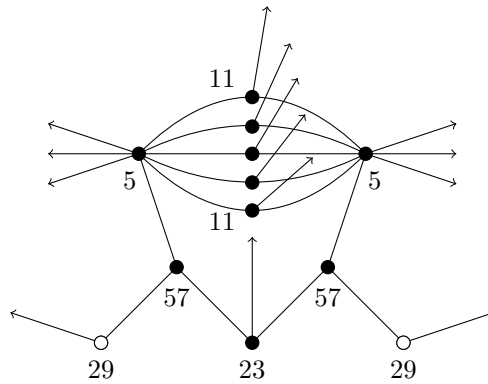


Figure 8.

multiplicity of  $\Pi_0$ , so it is the denominator  $d$  of the last characteristic Puiseux exponent of  $\Delta_0$ . Considering the restriction  $\ell|_{\Pi_0}: \Pi_0 \rightarrow \Delta_0$ , we obtain that  $d$  divides the multiplicity of the generic linear form at the exceptional curve intersecting  $\Pi_0^*$ , which can be read in Figure 7. This gives a bound on  $d$ , which enables one to compute the Puiseux expansion of all the branches  $\Delta$  using, for example, Maple. We obtain that  $\Delta$  decomposes as follows:

- Three branches  $\Delta_1, \Delta_2$  and  $\Delta_3$  tangent to the same line  $L_1$ , each with a single characteristic Puiseux exponent,  $\frac{6}{5}, \frac{6}{5}$  and  $\frac{5}{4}$ , respectively, and Puiseux expansions

$$\begin{aligned} \Delta_1: u &= av + bv^{6/5} + cv^{7/5} + \dots, \\ \Delta_2: u &= av + b'v^{6/5} + c'v^{7/5} + \dots, \\ \Delta_3: u &= av + b''v^{5/4} + c''v^{3/2} + \dots \end{aligned}$$

- For each  $i=2, \dots, 6$ , one branch tangent to  $L_i = \{(u, v): u = a_i v\}$  with  $\frac{3}{2}$  as single characteristic Puiseux exponent:  $u = a_i v + b_i v^{3/2} + \dots$

- Six branches, each lifting to a component of the polar whose strict transform meets one of the two  $\mathcal{L}$ -curves at a smooth point (these are “moving polar components” in the terminology introduced in the proof of Lemma 6.2(1)). So these do not contribute to the bilipschitz geometry.

The lines  $L_2, \dots, L_6$  correspond to the five thin zones coming from the five one-vertex Tjurina components (compare with Lemma 3.7). These five vertices are thus  $\mathcal{A}$ -nodes with rate equal to the characteristic Puiseux exponent  $\frac{3}{2}$ .

The line  $L_1$  is the projection of the exceptional line tangent to the thin piece  $Z_1$  associated with the big Tjurina component  $\Gamma_1$ . In order to compute the rate  $q_\nu$  at each node  $\nu$  of  $\Gamma_1$ , we would have to study explicitly the restriction of the cover  $\ell$  to  $Z_1$  over a carousel decomposition of its image and the reduction to the bilipschitz model, as in §13. The following remark will enable one to circumvent this technical computation.

*Remark 15.3.* Let  $\ell=(z_1, z_2): (X, 0) \rightarrow (\mathbb{C}, 0)$  be a generic linear projection. Denote by  $(u, v)=(z_1, z_2)$  the coordinates in the target  $\mathbb{C}^2$ . Let  $\Gamma_j$  be a Tjurina component of  $\Gamma$  and let  $\Pi_j$  be a branch of the polar curve of  $\ell$  contained in the thin piece  $Z_j$ . Suppose the branch  $\Delta_j=\ell(\Pi_j)$  of the discriminant curve has a single characteristic Puiseux exponent  $p$ , so the Puiseux expansion of  $\Delta_j$  is of the form

$$v = a_1u + a_2u^2 + \dots + a_ku^k + bu^ps + \dots,$$

where  $k$  is the integral part of  $p$  and  $b \neq 0$ . We perform the change of variable

$$v' = v - \sum_{i=1}^k a_i u^i.$$

In other words, we consider the projection  $(z_1, z'_2)$  instead of  $(z_1, z_2)$ , where

$$z'_2 = z_2 - \sum_{i=1}^k a_i z_1^i.$$

This projection has the same polar and discriminant curve as  $\ell$ , and in the new coordinates the Puiseux expansion of  $\Delta_j$  is  $v' = bu^p$ . Let  $\nu$  be a node in  $\Gamma_j$  such that  $\Pi_j \subset M_\nu$ , i.e.  $q_\nu = p$ . Then, according to [20] and [27], we have

$$p = \frac{m_\nu(z'_2)}{m_\nu(z_1)}.$$

The quotient  $m_\nu(z'_2)/m_\nu(z_1)$  is called the *Hironaka number* of  $\nu$  (with respect to the projection  $(z_1, z'_2)$ ).

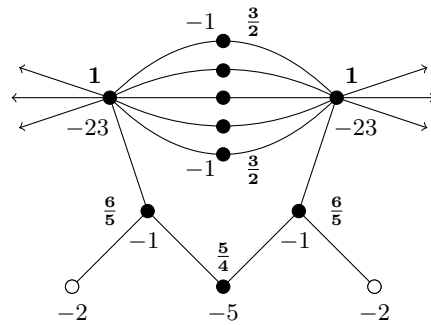
We return to the example. Since each branch  $\Delta_1, \Delta_2$  and  $\Delta_3$  has a single characteristic exponent and no inessential exponent before it in the expansion, we can apply the remark above. We use  $z'_2=x+y$ . Let  $E_1, \dots, E_5$  be the exceptional curves associated with the vertices of the big Tjurina component indexed from left to right. We first compute the multiplicities of  $z_1, x$  and  $y$  along the exceptional curves  $E_i$ . Then  $z'_2=x+y$  is a generic linear combination of  $x$  and  $y$ , and we obtain its multiplicities as the minimum of that of  $x$  and  $y$  on each vertex:

	$E_1$	$E_2$	$E_3$	$E_4$	$E_5$
$z_1$ :	5	10	4	10	5
$x$ :	7	13	5	12	6
$y$ :	6	12	5	13	7
$x+y$ :	6	12	5	12	6

Therefore the Hironaka numbers at the vertices of the Tjurina component  $\Gamma_1$  are

$E_1$	$E_2$	$E_3$	$E_4$	$E_5$
$\frac{6}{5}$	$\frac{6}{5}$	$\frac{5}{4}$	$\frac{6}{5}$	$\frac{6}{5}$

We thus obtain that the rates at the two  $\mathcal{T}$ -nodes equal  $\frac{6}{5}$ , and that the vertex in the middle is an  $\mathcal{A}$ -node with rate  $\frac{5}{4}$ . The bilipschitz geometry of  $(X, 0)$  is then given by the following graph (the rate at each node is written in boldface):



We now describe the same example via its carrousel. The carrousel sections for the six thin zones are illustrated somewhat schematically in Figure 9. They consist of five carrousel sections  $D_1, \dots, D_5$  for the five small thin zones containing components of the discriminant with Puiseux expansions of the form  $y=a_ix+b_ix^{3/2}+\dots$  and one carrousel section  $D_6$  for the “large” thin zone containing two components of the discriminant of the form  $y=cx+d_ix^{6/5}+\dots, i=1, 2$ , and one of the form  $y=cx+ex^{5/4}$ . There are also

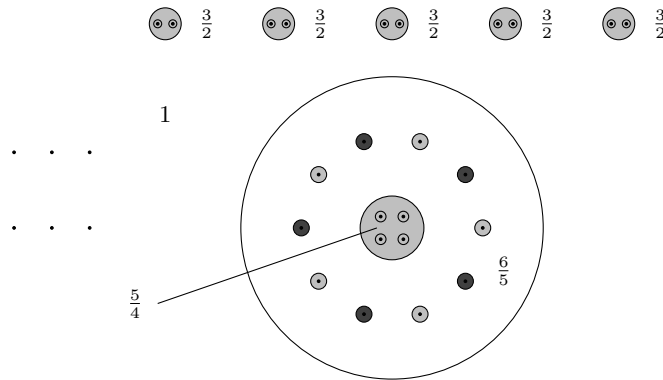


Figure 9.

six points representing the intersection points of components of the discriminant coming from the six moving polars in the thick zone.

For each  $i=1, \dots, 5$ ,  $\ell^{-1}(D_i)$  consists of an annulus which is a double branched cover of  $D_i$  and four disks, each of which simply covers  $D_i$  (the total degree must be the multiplicity of  $X$ , which is 6). So, for each  $i=1, \dots, 5$ , we see a special annular piece between the two thick zones plus four  $D$ -pieces, two contributing to each of the two thick zones. The carousel section  $D_6$  for the “large” thin zone represents two overlapping  $B$ -pieces with rate  $\frac{6}{5}$  connecting to a piece with rate  $\frac{5}{4}$  inside. Note that  $\ell^{-1}(D_6)$  consists of two disks and a surface  $F$  of genus 5 which four-fold covers  $D_6$ . The two disks correspond again to two  $D$ -pieces which contribute to the thick zones, while the surface  $F$  is made up of two annuli over the inner disk of  $D_6$  connecting to two surfaces of genus 2 over the outer annulus of  $D_6$ . The two annuli are in fact two sections by the Milnor fiber of a single special annular piece of rate  $\frac{5}{4}$  connecting the two pieces of rate  $\frac{6}{5}$  to form the “large” thin zone.

*Example 15.4.* (Simple singularities) The bilipschitz geometry of the  $A$ - $D$ - $E$  singularities is given in Table 10. The right column gives the numbers of thin pieces and thick pieces. According to Corollary 7.11, when  $(X, 0)$  does not have a thin piece, then it has a single thick piece and  $(X, 0)$  is metrically conical. Otherwise  $(X, 0)$  is not metrically conical.

*Example 15.5.* (Hirzebruch–Jung singularities) The Hirzebruch–Jung singularities (surface cyclic quotient singularities) were described by Hirzebruch as the normalizations of the singularities  $(Y, 0)$  with equation  $z^p - x^{p-q}y = 0$  in  $\mathbb{C}^3$ , where  $1 \leq q < p$  are coprime positive integers. The link of the normalization  $(X, p)$  of  $(Y, 0)$  is the lens space  $L(p, q)$

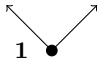
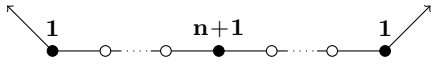
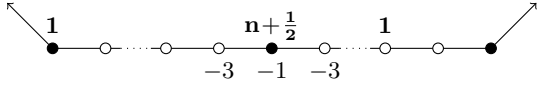
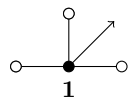
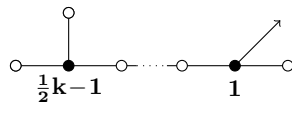
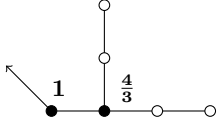
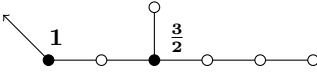
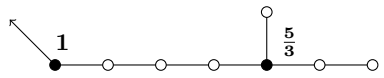
Singularity	bilipschitz geometry	thick-thin pieces
$A_1$		metrically conical
$A_{2n+1}, n \geq 1$		2 thick, 1 thin
$A_{2n}, n \geq 1$		2 thick, 1 thin
$D_4$		metrically conical
$D_k, k \geq 5$		1 thick, 1 thin
$E_6$		1 thick, 1 thin
$E_7$		1 thick, 1 thin
$E_8$		1 thick, 1 thin

Table 10. Bilipschitz geometry of simple singularities.

(see [12] and [14]) and the minimal resolution graph is a bamboo

$$\begin{array}{ccc} -b_1 & -b_2 & \dots & -b_n \\ \circ & \text{---} & \circ & \text{---} & \dots & \text{---} & \circ \end{array}$$

where  $p/q=[b_1, b_2, \dots, b_n]$ . The thick-thin decomposition of  $(X, 0)$  has been already described in the proof of Theorem 7.5: the generic linear form has multiplicity 1 along each  $E_i$ , and the  $\mathcal{L}$ -nodes are the two extremal vertices of the bamboo and any vertex with  $b_i \geq 3$ . To get the adapted resolution graph of §2 we blow up once between any two adjacent  $\mathcal{L}$ -nodes. Then the subgraph  $\Gamma_j$  associated with a thin piece  $Z_j$  is either a  $(-1)$ -weighted vertex or a maximal string  $\nu_i, \nu_{i+1}, \dots, \nu_k$  of  $(-2)$ -weighted vertices excluding  $\nu_1$  and  $\nu_n$ . There are no  $\mathcal{T}$ -nodes, so each Tjurina component is an  $\mathcal{A}$ -string giving a special annulus. The rate of the special annulus is  $\frac{3}{2}$  if the Tjurina component is a  $(-1)$ -vertex and  $\frac{1}{2}(m+3)$  for a string of  $m$   $(-2)$ -vertices.

*Example 15.6.* (Cusp singularities) Let  $(X, 0)$  be a cusp singularity [13]. The dual graph of the minimal resolution of  $(X, 0)$  consists of a cycle of rational curves with Euler weights  $\leq -2$  and at least one weight  $\leq -3$ . Since such a singularity is taut, its maximal cycle coincides with its fundamental cycle, and the generic linear form has multiplicity 1 along each irreducible component  $E_i$ . Therefore, the  $\mathcal{L}$ -nodes are the vertices which carry Euler class  $\leq -3$ , and the argument is now similar to the lens space case treated above: we blow up once between any two adjacent  $\mathcal{L}$ -nodes. Then the subgraph  $\Gamma_j$  associated with a thin piece  $Z_j$  is either a  $(-1)$ -weighted vertex or a maximal string  $\nu_i, \nu_{i+1}, \dots, \nu_k$  of  $(-2)$ -weighted vertices. As the distance  $\varepsilon$  to the origin goes to zero, we then see the link  $X^{(\varepsilon)}$  as a “necklace” of thick zones separated by thin zones, each of the latter vanishing to a circle. Again, the thin zones are special annuli with rates as in the previous example.

*Example 15.7.* (Briançon–Speder examples) The Briançon–Speder example we will consider is the  $\mu$ -constant family of singularities

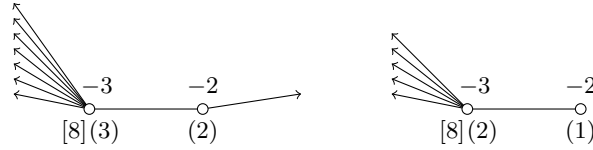
$$x^5 + z^{15} + y^7 z + txy^6 = 0,$$

depending on the parameter  $t$ . We will see that the bilipschitz geometry changes very radically when  $t$  becomes 0 (the same is true for the other Briançon–Speder families).

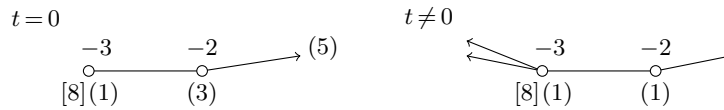
The minimal resolution graph of  $(X, 0)$  is

$$\begin{array}{ccc} -3 & & -2 \\ \circ & \text{---} & \circ \\ [8] & & \end{array}$$

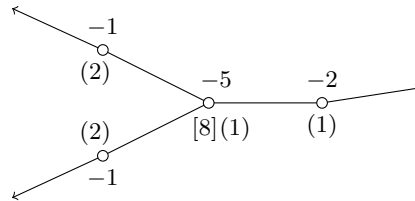
For any  $t$  the curves  $x=0$  and  $y=0$  are



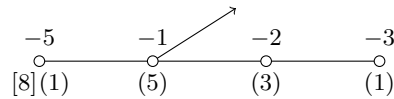
The curve  $z=0$  is



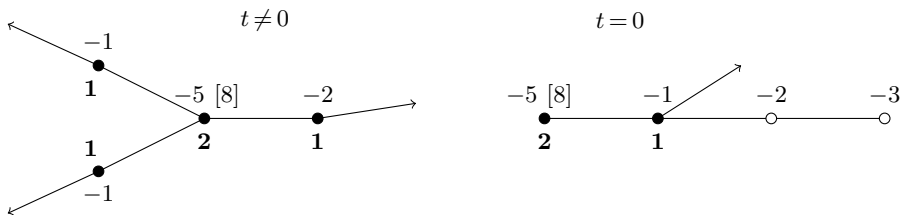
A generic linear form for  $t \neq 0$  is  $z=0$ , given by the right-hand graph above. To resolve the linear system of hyperplane sections one must blow up twice at the left node, giving three  $\mathcal{L}$ -nodes



The generic linear form for  $t=0$ , with the linear system of hyperplane sections resolved, is



So there is just one  $\mathcal{L}$ -node, and it is equal to neither of the original vertices of the resolution. We compute the rate at the  $\mathcal{T}$ -node from the Puiseux expansion of the branches of  $\Delta$ , and we obtain the following bilipschitz description:



## References

- [1] BERNIG, A. & LYCHAK, A., Tangent spaces and Gromov–Hausdorff limits of subanalytic spaces. *J. Reine Angew. Math.*, 608 (2007), 1–15.
- [2] BIRBRAIR, L. & FERNANDES, A., Inner metric geometry of complex algebraic surfaces with isolated singularities. *Comm. Pure Appl. Math.*, 61:11 (2008), 1483–1494.
- [3] BIRBRAIR, L., FERNANDES, A. & NEUMANN, W. D., Bi-Lipschitz geometry of weighted homogeneous surface singularities. *Math. Ann.*, 342 (2008), 139–144.
- [4] — Bi-Lipschitz geometry of complex surface singularities. *Geom. Dedicata*, 139 (2009), 259–267.
- [5] — Separating sets, metric tangent cone and applications for complex algebraic germs. *Selecta Math.*, 16 (2010), 377–391.
- [6] BOUTOT, J.-F., Singularités rationnelles et quotients par les groupes réductifs. *Invent. Math.*, 88 (1987), 65–68.
- [7] BRIANÇON, J. & HENRY, J. P. G., Équisingularité générique des familles de surfaces à singularité isolée. *Bull. Soc. Math. France*, 108 (1980), 259–281.
- [8] DURFEE, A. H., Neighborhoods of algebraic sets. *Trans. Amer. Math. Soc.*, 276 (1983), 517–530.
- [9] EISENBUD, D. & NEUMANN, W., *Three-Dimensional Link Theory and Invariants of Plane Curve Singularities*. Annals of Mathematics Studies, 110. Princeton University Press, Princeton, NJ, 1985.
- [10] FERNANDES, A., Topological equivalence of complex curves and bi-Lipschitz homeomorphisms. *Michigan Math. J.*, 51 (2003), 593–606.
- [11] GONZALEZ-SPRINBERG, G., Résolution de Nash des points doubles rationnels. *Ann. Inst. Fourier (Grenoble)*, 32:2 (1982), 111–178.
- [12] HIRZEBRUCH, F., Über vierdimensionale Riemannsche Flächen mehrdeutiger analytischer Funktionen von zwei komplexen Veränderlichen. *Math. Ann.*, 126 (1953), 1–22.
- [13] — Hilbert modular surfaces. *Enseign. Math.*, 19 (1973), 183–281.
- [14] HIRZEBRUCH, F., NEUMANN, W. D. & KOH, S. S., *Differentiable Manifolds and Quadratic Forms*. Lecture Notes in Pure and Applied Mathematics, 4. Marcel Dekker, New York, 1971.
- [15] HOCHSTER, M. & ROBERTS, J. L., Rings of invariants of reductive groups acting on regular rings are Cohen–Macaulay. *Adv. Math.*, 13 (1974), 115–175.
- [16] HSIANG, W. C. & PATI, V.,  $L^2$ -cohomology of normal algebraic surfaces. I. *Invent. Math.*, 81 (1985), 395–412.
- [17] JACO, W. H. & SHALEN, P. B., Seifert fibered spaces in 3-manifolds. *Mem. Amer. Math. Soc.*, 21 (1979).
- [18] KÄHLER, E., Über die Verzweigung einer algebraischen Funktion zweier Veränderlichen in der Umgebung einer singulären Stelle. *Math. Z.*, 30 (1929), 188–204.
- [19] LÊ DŨNG TRÁNG, The geometry of the monodromy theorem, in *C. P. Ramanujam—A Tribute*, Tata Inst. Fund. Res. Studies in Math., 8, pp. 157–173. Springer, Berlin–Heidelberg, 1978.
- [20] LÊ DŨNG TRÁNG, MAUGENDRE, H. & WEBER, C., Geometry of critical loci. *J. London Math. Soc.*, 63 (2001), 533–552.
- [21] LÊ DŨNG TRÁNG, MICHEL, F. & WEBER, C., Courbes polaires et topologie des courbes planes. *Ann. Sci. École Norm. Sup.*, 24 (1991), 141–169.
- [22] LÊ DŨNG TRÁNG & TEISSIER, B., Variétés polaires locales et classes de Chern des variétés singulières. *Ann. of Math.*, 114 (1981), 457–491.



- [23] — Limites d'espaces tangents en géométrie analytique. *Comment. Math. Helv.*, 63 (1988), 540–578.
- [24] LUENGO, I., The  $\mu$ -constant stratum is not smooth. *Invent. Math.*, 90 (1987), 139–152.
- [25] LUENGO, I., MELLE-HERNÁNDEZ, A. & NÉMETHI, A., Links and analytic invariants of superisolated singularities. *J. Algebraic Geom.*, 14 (2005), 543–565.
- [26] MENDRIS, R. & NÉMETHI, A., The link of  $\{f(x, y) + z^n = 0\}$  and Zariski's conjecture. *Compos. Math.*, 141 (2005), 502–524.
- [27] MICHEL, F., Jacobian curves for normal complex surfaces, in *Singularities II*, Contemp. Math., 475, pp. 135–150. Amer. Math. Soc., Providence, RI, 2008.
- [28] MICHEL, F., PICHON, A. & WEBER, C., The boundary of the Milnor fiber for some non-isolated singularities of complex surfaces. *Osaka J. Math.*, 46 (2009), 291–316.
- [29] MILNOR, J., *Singular Points of Complex Hypersurfaces*. Annals of Mathematics Studies, 61. Princeton University Press, Princeton, NJ, 1968.
- [30] MOSTOWSKI, T., Lipschitz equisingularity. *Dissertationes Math. (Rozprawy Mat.)*, 243 (1985).
- [31] — Tangent cones and Lipschitz stratifications, in *Singularities* (Warsaw, 1985), Banach Center Publ., 20, pp. 303–322. PWN, Warsaw, 1988.
- [32] NAGASE, M., Remarks on the  $L^2$ -cohomology of singular algebraic surfaces. *J. Math. Soc. Japan*, 41 (1989), 97–116.
- [33] NEUMANN, W. D., A calculus for plumbing applied to the topology of complex surface singularities and degenerating complex curves. *Trans. Amer. Math. Soc.*, 268 (1981), 299–344.
- [34] NEUMANN, W. D. & SWARUP, G. A., Canonical decompositions of 3-manifolds. *Geom. Topol.*, 1 (1997), 21–40.
- [35] PARUSIŃSKI, A., Lipschitz properties of semi-analytic sets. *Ann. Inst. Fourier (Grenoble)*, 38:4 (1988), 189–213.
- [36] — Lipschitz stratification of subanalytic sets. *Ann. Sci. École Norm. Sup.*, 27 (1994), 661–696.
- [37] PEDERSEN, H. M., Classifying metrically conical rational singularities. Preprint, 2011. [arXiv:1112.0125 \[AG\]](https://arxiv.org/abs/1112.0125).
- [38] PHAM, F. P. & TEISSIER, B., Fractions Lipschitziennes d'une algèbre analytique complexe et saturation de Zariski. Prépublications École Polytechnique No. M17.0669. Paris, 1969.
- [39] PICHON, A., Fibrations sur le cercle et surfaces complexes. *Ann. Inst. Fourier (Grenoble)*, 51:2 (2001), 337–374.
- [40] ROUSSARIE, R., Plongements dans les variétés feuilletées et classification de feuilletages sans holonomie. *Inst. Hautes Études Sci. Publ. Math.*, 43 (1974), 101–141.
- [41] SIEBENMANN, L. & SULLIVAN, D., On complexes that are Lipschitz manifolds, in *Geometric Topology* (Athens, GA, 1977), pp. 503–525. Academic Press, New York, 1979.
- [42] SNOUSSI, J., Limites d'espaces tangents à une surface normale. *Comment. Math. Helv.*, 76 (2001), 61–88.
- [43] SPIVAKOVSKY, M., Sandwiched singularities and desingularization of surfaces by normalized Nash transformations. *Ann. of Math.*, 131 (1990), 411–491.
- [44] STALLINGS, J., On fibering certain 3-manifolds, in *Topology of 3-Manifolds and Related Topics* (Proc. The Univ. of Georgia Institute, 1961), pp. 95–100. Prentice-Hall, Englewood Cliffs, NJ, 1962.
- [45] TEISSIER, B., Variétés polaires. II. Multiplicités polaires, sections planes, et conditions de Whitney, in *Algebraic Geometry* (La Rábida, 1981), Lecture Notes in Math., 961, pp. 314–491. Springer, Berlin–Heidelberg, 1982.

- [46] THURSTON, W. P., *Foliations of 3-Manifolds which are Circle Bundles*. Ph.D. Thesis, University of California, Berkeley, 1972.
- [47] VALETTE, G., The link of the germ of a semi-algebraic metric space. *Proc. Amer. Math. Soc.*, 135:10 (2007), 3083–3090.
- [48] WALDHAUSEN, F., On irreducible 3-manifolds which are sufficiently large. *Ann. of Math.*, 87 (1968), 56–88.

LEV BIRBRAIR  
Departamento de Matemática  
Universidade Federal do Ceará  
Campus do Picici, Bloco 914  
Cep. 60455-760. Fortaleza-Ce  
Brasil  
[birb@ufc.br](mailto:birb@ufc.br)

WALTER D. NEUMANN  
Department of Mathematics  
Barnard College  
Columbia University  
2990 Broadway MC4429  
New York, NY 10027  
U.S.A.  
[neumann@math.columbia.edu](mailto:neumann@math.columbia.edu)

ANNE PICHON  
Aix Marseille Université  
CNRS, Centrale Marseille  
I2M, UMR 7373  
FR-13453 Marseille  
France  
[anne.pichon@univ-amu.fr](mailto:anne.pichon@univ-amu.fr)

*Received January 19, 2012*

*Received in revised form June 21, 2013*